NTNU
Norwegian University of
Science and Technology

Investigation of resistivity, porosity and pore solution composition in carbonated mortar prepared with ordinary Portland cement and Portland-fly ash cement

Simon Liseth Langedal

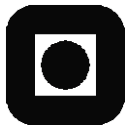**Department of Structural Engineering**
Faculty of Engineering Science and Technology
NTNU- Norwegian University of Science and Technology

ACCESSIBILITY

OPEN

MASTER THESIS 2018

SUBJECT AREA:	DATE:	NO. OF PAGES:
Concrete Technology	14.01.2018	67

TITLE:

Investigation of resistivity, porosity and pore solution composition in carbonated mortar prepared with ordinary Portland cement and Portland-fly ash cement

Undersøkelse av resistivitet, porøsitet og porevannssammensetningen i karbonatisert mørtel laget med ordinær Portland sement of Portland flyveaske sement.

BY:

Simon Liseth Langedal

SUMMARY:
This project investigated how carbonation affected resistivity in mortars made with different cement types. The goal was to explain this by investigating the pore solution composition, the pore structure and the moisture content in mortars made with different cements and exposed to different relative humidity and CO_2-concentrations. Mortar samples made with CEM I and CEM II/B-V were cured for 14 days and exposed to CO_2 for 27 weeks before testing. The resistivity was measured using embedded titanium bars in the mortar samples. The pore structure was investigated using the PF-method. The extent of carbonation was measured using thermogravimetric analysis. The pore solution composition was investigated with cold water extraction and pore solution expression followed by analysis by ICP-MS. The impact of carbonation in the different RH-conditions could not be concluded, as the mortars stored at 90% RH and 5% CO_2 had not fully carbonated within the course of the project. Carbonation caused the resistivity to increase drastically for both cement types. The resistivity of mortars made with CEM II/B-V were found to be higher than that of mortars made with CEM I, both in carbonated and non-carbonated state, but the ratio between the two cements could indicate that carbonation may have a bigger impact on the resistivity than the type of cement has. Carbonation decreased the moisture content and pore volume in the mortars from both cement types. The mortars made with CEM II/B-V showed a larger pore volume than mortars made with CEM I in all exposure conditions. The degree of capillary saturation was found to be related to resistivity, as a lower degree of saturation corresponded to a higher resistivity. The pore solution composition also changed upon carbonation. A significant drop in the concentration of Na and K was seen upon carbonation. In the non-carbonated samples, the samples from CEM I showed a higher content of Na and K compared to samples from CEM II/B-V, whereas the Na and K content was similar for both cement types after carbonation.

Both moisture content, degree of capillary saturation and pore solution composition appears to influence the resistivity, but it was not possible to conclude to which extent each parameter influenced the resistivity.

RESPONSIBLE TEACHER: Klaartje De Weerdt

SUPERVISOR(S): Andres Belda Revert, Klaartje De Weerdt & Mette Rica Geiker

CARRIED OUT AT: Department of Structural Engineering - Norwegian University of Science and Technology

Investigation of resistivity, porosity and pore solution composition in carbonated mortar prepared with ordinary Portland cement and Portland-fly ash cement

Simon Liseth Langedal

14.01.2018

MASTER THESIS
Department of Structural Engineering
Norwegian University of Science and Technology

Supervisor 1: Andres Belda Revert

Supervisor 2: Klaartje De Weerdt

Supervisor 3: Mette Rica Geiker

Preface

This project is the result of my work with the master thesis course "TKT4925 - Betongteknologi, masteroppgave" at the Norwegian University of Science and Technology. This course accounts for 30 ECTS credits. The work was carried out by me, Simon Liseth Langedal, in cooperation with supervisors, between August 2017 and January 2018.

In the spring of 2017 i wrote my project thesis on the same subject as I have now written my master thesis. The project you currently are reading is the result of both the casting and preparations done in my project thesis, and the testing and investigations done in my master thesis.

Before determining the area I wanted to investigate, I worked as a research assistant at NTNU with Andres Belda Revert under his PhD, NFR project no. 235211/O30: Development of low-carbon cement for concrete building structures with excellent durability "Lavkarbsem" Subproject 2B "Residual Service Life", and was through this introduced to carbonation and corrosion in concrete. I found it interesting, and decided to write this project on how different cements are affected by carbonation.

My supervisors for this project are PhD student Andres Belda Revert, associate professor Klaartje De Weerdt and professor Mette Rica Geiker from NTNU.

Trondheim, 14-01-2018

Simon Liseth Langedal

Acknowledgment

I would like to thank Andres Belda Revert for his help during this project. He has been a great contributor during all the phases of this project, from providing relevant background information to helping with the casting and implementing of the practical work in the lab. Andres has helped me write a much more thorough thesis than I could have managed on my own. I hope that my thesis can provide some results in his work with his PhD.

I would also like to thank Klaartje De Weerdt and Mette Rica Geiker for supervising my project, and for making time for discussions and follow up on my work.

<div align="right">S.L.L</div>

Summary

The goal of this project was to investigate how carbonation affects resistivity in mortars made with different cement types. The goal was to explain this by investigating the pore solution composition, the pore structure and the moisture content in mortars made with different cements and exposed to different relative humidity and CO_2-concentrations. It was used two different cements, CEM I (regular Portland cement) and CEM II/B-V (Portland fly ash cement). The samples were stored at two different CO_2-concentrations and relative humidity's; 1 % CO_2 with 60 % RH, and 5 % CO_2 with 90 % RH. All the carbonating samples had reference samples stored at 0 % CO_2. The samples were cured for 14 days and exposed to CO_2 for 27 weeks before testing. The samples were casted in bottles with diameter 50 mm and sawn into discs with 15 mm height after curing.

The resistivity was measured using embedded titanium bars in the mortar samples. The pore structure was investigated using the PF-method. The extent of carbonation was measured using thermogravimetric analysis. The pore solution composition was investigated with cold water extraction and pore solution expression followed by analysis by ICP-MS.

Due to the low extent of carbonation in the samples stored in 90 % RH and 5 % CO_2, this thesis could not show the relationship between the resistivity of carbonated samples at different RH.

The resistivity of mortars made with CEM II/B-V were found to be higher than mortars made with CEM I, by a factor of 1.8 in carbonated state and by a factor of 5.6 in non-carbonated state. The resistivity was significantly higher in carbonated mortar than non-carbonated mortar for both cements. The ratio of resistivity between CEM I and CEM II/B-V was smaller in the carbonated state than the non-carbonated state, indicating that carbonation may have a greater impact on resistivity than the type of cement has.

Carbonation decreased the moisture content and pore volume in the mortars from both cement types. The mortars made with CEM II/B-V showed a larger pore volume than mortars made with CEM I in all exposure conditions. The degree of capillary saturation was related to the resistivity,as a lower degree of saturation corresponded to a higher resistivity. The pore solution composition changed upon carbonation. A significant drop in the concentration of Na and K was seen upon carbonation. In the non-carbonated samples, the samples from CEM I showed a higher content of Na and K compared to samples from CEM II/B-V, whereas the Na and K content was similar for both cement types after carbonation.

Both moisture content, degree of capillary saturation and pore solution composition appears to influence the resistivity, but it was not possible to conclude to which extent each parameter influenced the resistivity.

Contents

List of Figures

List of Tables

1   Introduction

1.1   General

Portland cement is the basis for the most commonly used concretes today [8]. It is produced by burning a mixture of limestone and clay, and then grinding the materials [8]. The production of cement emits a large amount of CO_2, 0.87 tons per ton cement produced [11]. In order to lower the CO_2-footprint in cement production, fly ash is often used as a supplementary cementitious material (SCM). Fly ash is a bi-product of coal fueled power plants [17], and is a pozzolanic material that reacts with the hydration products.

When cement reacts with water, different hydration products are introduced. Hydration of calcium silicates produces calcium hydroxide, $Ca(OH)_2$, which together with NaOH and KOH cause the high pH found in hydrated cements [8].

1.2   Carbonation

In the process of carbonation, CO_2 penetrates the concrete through the pores and dissolves in the pore water. The CO_2 then reacts with the different hydration products, causing a pH drop in the pore solution, as low as 7.2 [2].

Carbonation of concrete causes no significant risk to the concrete itself, but is a major threat to the concrete reinforcement bars. In non-carbonated concrete, the pH is high and a passive film surrounds the reinforcement. When the pH is lowered, the protective film around the rebars dissolves and corrosion may occur with the presence of oxygen and humidity [14].

Carbonation causes changes in concrete. In addition to the lowering of pH, carbonation will alter the pore-structure, as the products formed during carbonation are different in volume compared to the original components. A change in the pore structure and pore solution composition will have an influence on concrete resistivity and the corrosion potential of the steel embedded in the concrete.

1.3   Background

In this section a brief introduction to the topics investigated is presented.

There is a large focus on corrosion of steel in concrete in the field of concrete technology. Carbonation of concrete is one of the main reasons for corrosion, and a number of papers have been written on topics regarding different factors affected by carbonation.

This project will focus on resistivity, pore solution composition, pore structure, corrosion potential of carbonated and non-carbonated mortars made with Portland cement and Portland fly ash cement (from now on referred to as CEM I and CEM II/B-V). The aim is to explain how these factors change upon carbonation, and how they are related to each other. The amount of literature on this subject is very limited. Is it possible to find the decisive factor on what controls the resistivity? The durability of concrete is strongly dependent on these factors, and showing the relationship between them could increase the understanding of deterioration mechanisms in concrete.

The investigation of the pore solution of concretes is an important part of concrete research [31]. By analyzing the pore solution before and after carbonation, it is possible to determine the change in pH and the composition of the solution. It is possible to determine which solid phases are stable, and which phases are unstable and may dissolve [31]. Analyzing the pore solution can increase the understanding of the chemical processes in hydrating cement [31].

Porosity and the pore structure determine the transport mechanisms in concrete. If a concrete develops large interconnected pores, water can "flow" easily through the concrete, carrying different ions. A denser, less permeable concrete, may be more resistant when it comes to penetration of gases and liquids. Carbonation has shown to alter the porosity of concrete, thereby changing the transport mechanisms.

Concrete resistivity is a material property that describes the electrical resistance. That is the ratio between applied voltage and resulting current [27], or how a material "slow down" the flow of electric current [16]. The electrical resistivity (ρ) is expressed as the product of electrical resistance (R) and a cell constant (k) [16]. The electrical resistance is the ratio of voltage (U) to current (I). The cell constant takes the geometry of the sample into account, and can be calculated numerically or by calibration using a material with known resistivity [16].

$$\rho = \left(\frac{U}{I}\right) \cdot k = R \cdot k \tag{1}$$

The current flows in the pore solution, "carried" by ions [27]. The pore solution composition also influence the resistivity, as a lower pH means less ions and a higher resistivity. This means that a concrete with large, interconnected pores has a lower resistivity than a denser concrete. Carbonated concrete has shown a higher resistivity [27],indicating that carbonation causes changes in the pore structure as well as in the pore solution composition.

When steel is corroding in concrete, an anodic and a cathodic reaction is taking place on the surface of the steel. At the anode, the corroding site, the iron is dissolved $Fe \rightarrow Fe^{2+} + 2e^-$. The electrons are consumed by the cathodic reaction $O_2 + 2H_2O + 4e^- \rightarrow 4OH^-$ [14]. With equipment

such as reference electrodes, it is possible to measure the corrosion potential of steel in concrete and indicate if the steel is corroding without breaking the sample open.

1.4   Objectives and research questions

The main goal of this project is to investigate how carbonation affects resistivity in mortars made with different cement types. We tried to explain the changes by investigating the pore solution composition, the pore structure and the moisture content in mortars made with different cements and exposed to different relative humidity and CO_2-concentrations.

The main questions this thesis will try to answer is:

- How resistivity changes upon carbonation

    - How different cement types and exposure conditions affecting the resistivity upon carbonation

- How porosity and moisture content change upon carbonation

    - How the change in porosity and moisture content developing in different cements and different exposure conditions

- How the pore solution composition change upon carbonation

    - How different cement types and exposure conditions affecting this change

- Which factor is dominant in the change of resistivity upon carbonation

    - How is the porosity and moisture content affecting the resistivity

    - How is the pore solution composition affecting the resistivity

In order to answer the research questions, a series of tests were performed. The main practical objectives was to first decide on the tests and then cast the necessary amount and types of samples in order to perform these tests. After casting and exposing the samples, the next step was to measure the resistivity in carbonated mortars in different moisture conditions, perform the PF-test to investigate the pore structure and moisture content in the samples, perform cold water extraction, pore solution extraction and analyze the pore solution through ICP-MS to investigate the pore solution composition, then compare the results with existing literature and show the relationship between the characteristics investigated. Two different mortars containing CEM I and CEM II/B-V were casted and placed in four different exposure environment. The environments differed in relative humidity and CO_2-concentration, and all the samples exposed

to CO_2 had reference samples stored in the same relative humidity but without the presence of CO_2.

1.5   Structure of the Report

In Chapter 2 different techniques and tests regarding the investigated factors are explained. There are also listed results and observations made by other authors. Chapter 3 is the experimental chapter, which describes all the samples casted, the exposure conditions, the tests performed and so on. All the results acquired in this thesis is listed in Chapter 4. In Chapter 5 all the results are discussed, compared with existing literature and parallels are drawn. The conclusion is in Chapter 6 and the recommendation for further research is in Chapter 7. The Appendix in Chapter A contains raw data and additional information regarding testing and calculations.

1.6   Limitations

During the work on this thesis, there have been some challenges. The work started out with a much wider scope and goal, and gradually this has shrunk to the objectives and goals written above. A lot of time has gone to figuring out solutions to problems or trying out different things that ultimately led to it not working. One example was trying to get samples to carbonate in 90 % RH. This was supposed to take 18 weeks, but after 26 weeks there was still no sign of full carbonation. Due to these limitations, I was not able to compare the effect of carbonation in different relative humidity conditions and at different CO_2-concentrations. The samples were crushed and left for another 8 weeks in exposure, run through TGA and compared to other samples that I knew were carbonated, and all this work resulted in confirming that the samples were not carbonated and could not be compared to the rest of my results.

Another limitation was the ability to extract pore solution from the CO_2-exposed samples. They appeared to be too dry to yield any solution, and another test had to be implemented. The original plan was to measure pH and resistivity in the pore solution, but this had to be changed since no pore solution was available.

When checking the carbonation front in the samples, it was discovered that they carbonated uneven, which indicated inhomogeneous samples. This was in contradiction to a investigation done during my project thesis, where the samples carbonated evenly and indicated a homogeneous material. This could cause error in measurements, and could also explain the large error bars in the corrosion potential and resistivity values. To a certain degree it could also explain why some samples carbonated faster than others.

The corrosion potential was investigated to check the relation between corrosion, moisture and resistivity upon carbonation. The results from these measurements gave no indication of the existence of such a relation, and is therefore not discussed.

All in all, there has been a lot of trial and error during the work on this thesis. I have spent hours upon hours in the lab just to confirm that something is not going to work. But spending so much time in the lab has also been interesting, and given me a much better understanding of the subjects in this thesis.

2 Theory on Tests and Techniques

There are different tests and trials that can be performed to investigate the effect of carbonation in concrete. This project will focus on tests that investigates resistivity, pore structure, corrosion potential and pore solution composition.

2.1 Resistivity

There are different ways to measure concrete resistivity, depending on the geometry of the sample, whether you are in the lab or in the field, or if you have embedded equipment or not. The principle of the different methods remains the same: to measure the ratio of voltage applied and current measured.

The value measured is the *resistance* of concrete. In order to calculate the *resistivity*, equation 1 must be applied.

Two-electrode systems is the most commonly used method to determine concrete resistivity in the lab [16]. The resistance is measured between two electrodes, placed outside, or embedded inside, a sample. Figure 1 show different setups for two-electrode systems.
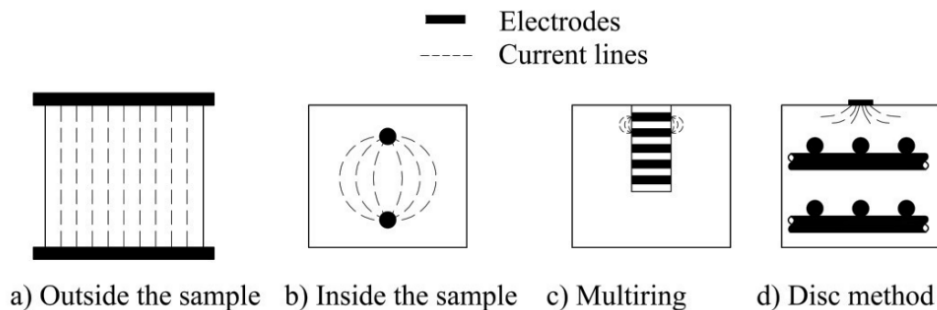
Figure 1: Two-electrode setups. From [16].

The electrodes can be of any conductive material, steel plates, rods, wires or reinforcement [16]. Another method for resistivity measurement is the four-electrode systems. This system is mostly used for field measurements. Current is sent between two outer electrodes, and a potential drop is measured between the two inner electrodes, determining the resistance [16].

When placing electrodes on concrete surfaces, contact between the concrete surface and the electrode is crucial. Contact is ensured by placing a wet cloth or sponge between the electrode and the concrete.

R. B. Polder [27] gives some reference values of concrete resistivity from different laboratory studies. This is shown in Table 1.

Table 1: From [27]: "*Global reference values at 20°C for the electrical resistivity of dense-aggregate concrete of mature structures age >10 years; conditions in square brackets are corresponding laboratory climates.*

Environment	Concrete resistivity ($\rho_{concrete}$) [Ω m]	
	Ordinary Portland cement (CEM I)	Blast furnace slag cement (>65% slag) or fly ash (>25%) or silica fume (>5%)
Very wet, submerged, splash zone, [fog room]	50–200	300–1000
Outside, exposed	100–400	500–2000
Outside, sheltered, coated, hydrophobised (not carbonated) [20°C/80%RH]	200–500	1000–4000
Ditto, carbonated	1000 and higher	2000–6000 and higher
Indoor climate (carbonated) [20°C/50%RH]	3000 and higher	4000–10 000 and higher

Resistivity measurements in concrete are being used as a method to evaluate the durability of concrete structures [4]. The durability of concrete can be described as its ability to resist aggressive gases and liquids [4]. The resistivity is therefore often used as an indicator of a concretes structure´s durability, since a high resistivity could indicate a high ability to resist penetration of aggressive media. There is though a lot of discussion between different authors regarding this relationship. Resistivity can also indicate the pore structure and the connectivity of the pores, which are important parameters in durability assessment [4].

Medeiros-Junior et al. (2016) [29] performed resistivity measurements over 2 years of unsaturated concrete samples made with different cements. Their findings show that the type of cement used greatly influenced the resistivity. They found that cements with additions such as fly ash had higher resistivity than cements without additions. The cements with additions also have the highest resistivity increase over time, due to the more aggressive hydration reaction in fly pozzolanic cements compared to pure cement clinker [29].

Moisture content has shown to have an effect on the resistivity of concrete, as ions transported

in the pore water is what drives the current through the concrete [16]. An ordinary saturated OPC has shown to have a resistivity between 10-100 Ωm, while dry concretes shows a resistivity of 10^6-10^7 Ωm [13].

Gjørv et al. (1977) [15] show the relationship between electrical resistivity and moisture content in PCC in Figure 2
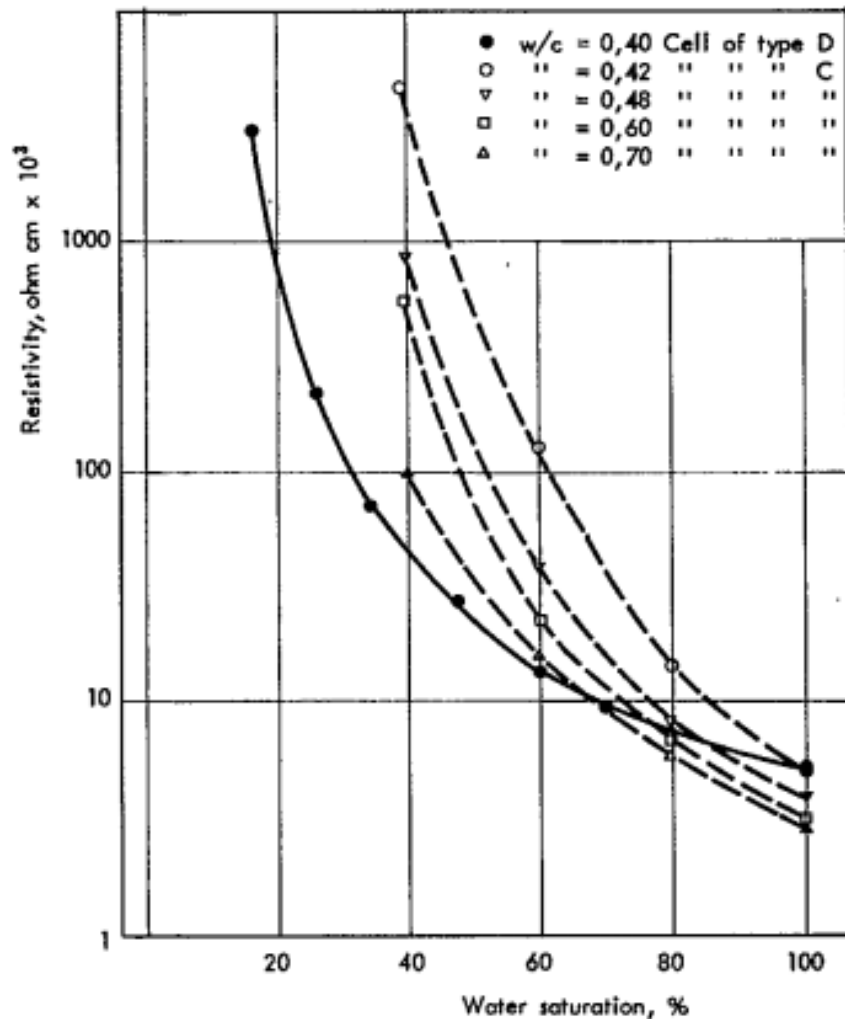
Figure 2: Effect of water saturation on resistivity of PCC. From [15]

2.2 Pore structure investigation

There are different investigation techniques to classify porosity, and these are often used in combination with each other in order to describe a concrete´s pore structure.

The PF-method estimates the volume of pores of different sizes in a sample. It is done by mea-

suring the amount of water in a sample by weighing it after drying and saturation. First, the sample is dried in an oven until all evaporable water is gone and dry weight is measured. Then the sample is re-saturated by submerging and weighted both in air and under water for volume determination. Finally, the sample is pressure saturated to access all pore sizes and weighted again. The total pore volume can now be determined from the fully saturated weight and the dry sample weight. The gel- and capillary pore volume can be derived from the amount of water taken in by the sample under natural suction by submerging. The in-situ moisture content can also be determined if the samples are weighted before the initial drying.

Mercury intrusion porosimetry (MIP) is a "*technique based on the intrusion of a nonwetting fluid (mercury) into porous structures under increasing pressure*" [6]. The idea is then to measure how much fluid a sample can take in, and under which pressure, in order to measure the size and volume of pores. One drawback of the MIP test is that the mercury only reaches the connected pores. The result will represent the pore *entry size* distribution, and not the *total pore size* distribution [6].

The gamma-ray attenuation method (GRAM) is a non-destructive test able to determine density in building materials [21]. GRAM has also been used to determine the carbonation front in concrete by measuring the density increase due to carbonation [21]. The test prinsiple is based on the absorption of gamma-rays emitted by a radioactive source.

Østnor et al. [30] performed tests regarding the carbonation mechanisms on pastes made with OPC and fly ash blends. They performed MIP on samples cured for 14 and 56 days and carbonated in 60 % RH. They show that non-carbonated fly ash cement has a higher total porosity than non-carbonated OPC. For the samples cured for 14 days, the porosity decreases in both cement pastes upon carbonation, but the effect is greater in OPC with a decrease of 10 %, compared to a 4 % decrease in porosity in fly ash cement paste. For the samples cured for 56 days, the porosity decreases with 4 % in OPC samples and with 2 % in fly ash samples upon carbonation.

Morandeau et al. [20] performed a series of tests regarding the porosity of carbonated CEM I based pastes and mortars. They use a combination of MIP and GRAM and state that the total porosity decreases with carbonation. They also show that the variation in porosity stays the same before and after carbonation, which means that carbonation has a clogging effect in the whole range of pores. The porosity measurements done by Morandeau et al. is shown in Figure 3. Morandeau et al. also performed tests on carbonated fly ash blended cement pastes [21]. They show that for pastes with a high amount of fly ash, above 30 %, and a water to binder ratio of above 0.6, the pastes develop coarser capillary pores even though the total porosity decreases. This indicates that fly ash affects the change in pore structure due to carbonation differently than regular Portland cement.
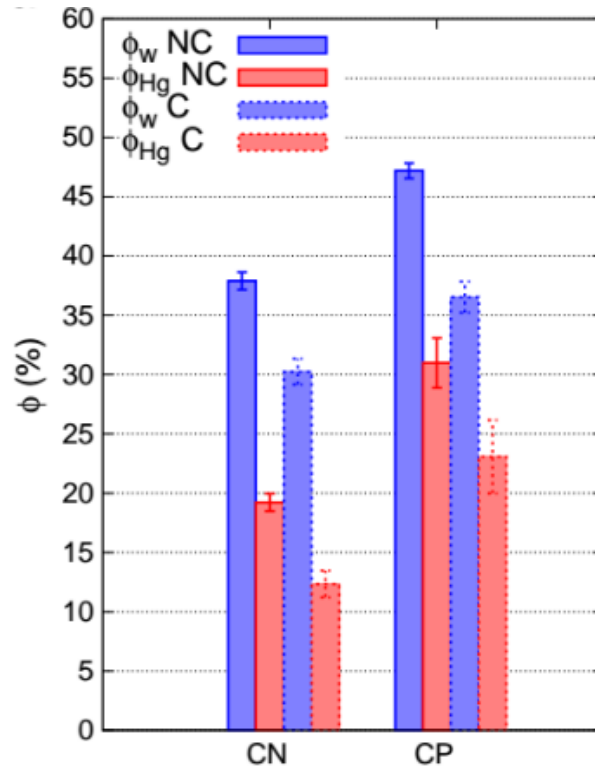
Figure 3: Total porosity measured with MIP ϕ_{Hg} and GRAM ϕ_w for carbonated (C) and non-carbonated (NC) cement pastes. From [20].

Pihlajavaara [24] performed tests regarding the change in porosity due to carbonation using MIP and surface area determination with the aid of water adsorption. Figure 4 show the porosity distribution of carbonated and non-carbonated mature cement pastes [24]. Finnish ordinary Portland cement was used in the trial [24]. This shows that the total porosity of carbonated cement is lower than for non-carbonated cement.
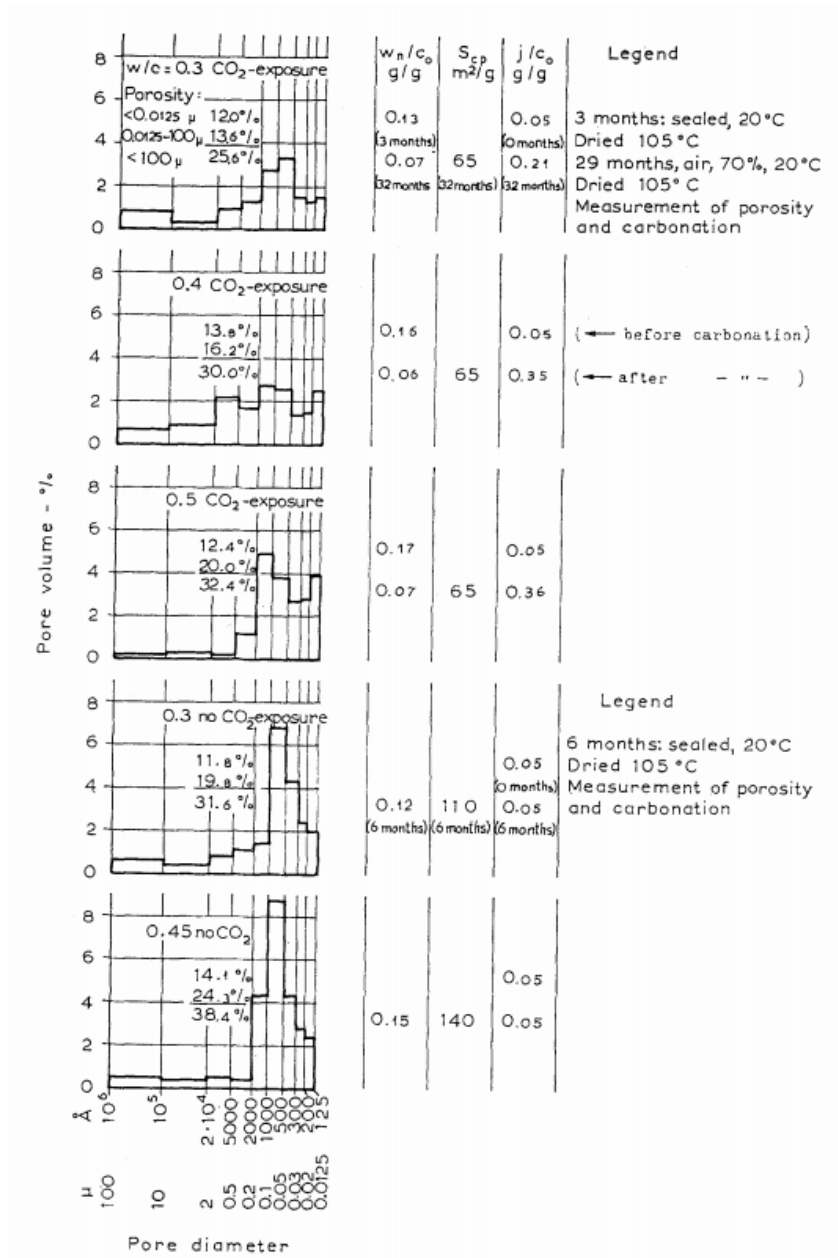
Figure 4: Porosity distribution and specific areas of carbonated and non-carbonated mature cement pasted. Figure from [24].

2.3 Corrosion potential

There are two types of corrosion for steel in concrete, uniform corrosion and pitting corrosion [14]. When dealing with a fully carbonated sample, all the steel is in the carbonated zone and therefore all of the protective oxide film is destroyed. This means that the whole steel surface is corroding, called uniform corrosion, where the anodic and cathodic reaction is located at the

same place, making a lot of micro-cells on the steel surface [14].

The corrosion potential is measured as the potential difference against a reference electrode, called a half-cell potential [14]. The measured values are dependent on a number of factors, such as moisture conditions, concrete cover and access to oxygen.

The test is done with different equipment, depending on the area investigated. For big slabs, rolling wheel electrodes can be used to map a large area [14]. Point measurements can be taken by a single electrode in a grid-pattern to map the corrosion potential. In small samples, one point of measurement can be used over a period of time to investigate the development of corrosion potential. The principle of the different testing is the same, a wire is connected to the steel in the concrete, and a reference electrode is placed on the concrete itself, creating a circuit as shown in Figure 5. The potential of steel in concrete are dependent on many factors. Some normal values are shown in Table 2.
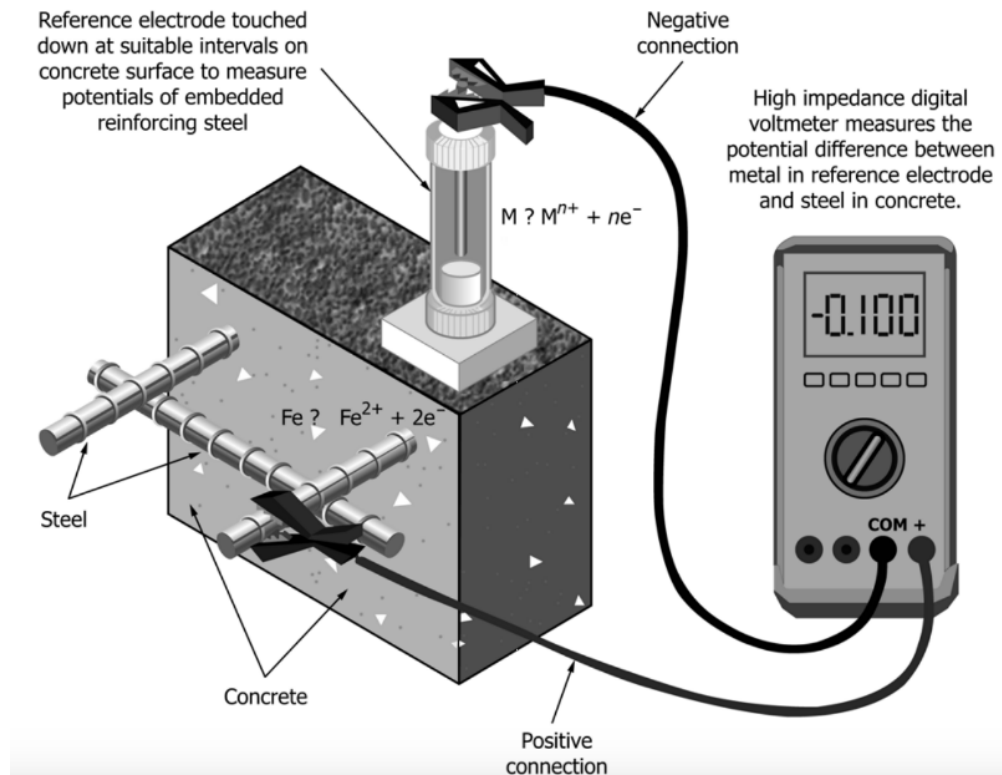
Figure 5: Reference electrode setup. From [3].

Table 2: From [14]. Typical ranges of potentials of carbon steel in concrete (Volts CSE)

Water saturated concrete without oxygen	[-0.9 , -1.0 V]
Wet, chloride contaminated concrete	[-0.4 , -0.6 V]
Humid, chloride free concrete	[+0.1 , -0.2 V]
Humid, carbonated concrete	[+0.1 , -0.4 V]
Dry, carbonated concrete	[+0.2 , 0 V]
Dry concrete	[+0.2 , 0 V]

2.4   Pore solution investigation

There are several techniques for analyzing the pore solution of concrete. Both destructive and non-destructive methods [5]. Destructive techniques means techniques that destroy the test-object.

Destuctive methods described in A. Behnood et al. [5] are the *expression method*, the *in-situ leaching method*, and the *ex-situ leaching method*.

The expression method (PSE) is a technique that presses the water out of the pores of a concrete sample, making it possible to analyze the composition of the pore solution directly [25]. In this test, a sample is placed under pressure in a devise shown in Figure 7. The devise is put under pressure, compacting the sample, and expressing the pore solution. The amount of pressure varies from study to study, but Vollpracht et al. [31] found that applying a pressure of 250 MPa is sufficient. On the other hand, Cyr et al. [9] carried out a trial on PSE using CEM I with water to cement ratio of 0.5 cured for 28 days under sealed conditions and 20°C. The samples were crushed and run through PSE with a loading sequence of 1 MPa/second (17 minutes per sample) and found that a pressure below 300 MPa was insufficient in order to obtain pore solution, as shown in Figure 6.

	Squeezing pressure (MPa)	Extracted pore solution (g)	Available pore solution ω (%)	Extraction efficiency E (%)	pH
Tests for repeatability[†]					
Mortar					
1a	1000	4.9	5.0	36.8	13.9
1b		4.9	5.1	37.4	13.7
1c		5.0	5.0	37.6	13.6
1d		5.1	5.2	39.2	13.8
1e		5.5	5.1	38.7	13.8
1f		5.1	5.2	39.3	13.8
Mortar					
2a		5.2	5.1	38.5	13.8
2b		4.8	5.1	36.0	13.8
2c		5.0	5.1	36.4	13.8
2d		5.7	5.0	41.7	13.8
2e		5.4	5.0	39.2	13.8
2f		5.2	5.0	38.5	13.8
Effect of squeezing pressure[‡]					
Mortar					
3a	300	0.0	6.7	0.0	N/A
3b	500	1.4	6.9	7.7	13.4
3c	750	4.9	7.1	26.0	13.4
3d	1000	7.3	7.5	36.9	13.4

[†]Storage in plastic bags at 20°C; [‡]Storage in water at 20°C

Figure 6: Amount of pore solution obtained at various pressure during PSE. Table from [9].
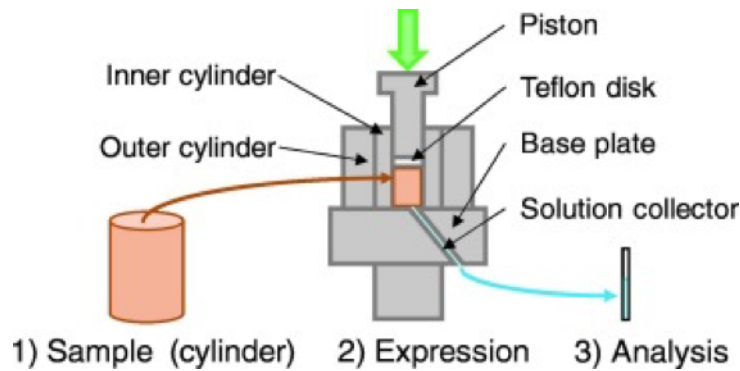
Figure 7: Pore solution expression. Figure from [25]

The in-situ leaching method is a technique for measuring pH in concrete. A 25 mm deep, 5 mm wide hole is drilled, the concrete powder removed, and deionized water is pipetted into the hole [5]. The pH is then measured by inserting a pH micro electrode and a reference electrode in the water. The potential difference is measured and converted to pH values [5]. This method

is relatively simple, but it requires some stabilization-time to obtain equilibrium in the solution and the surrounding concrete.

Ex-situ leaching is a method that is almost opposite of the in-situ leaching method. In this test, a given amount of powder drilled from a concrete sample is mixed with deionized water and analyzed. The filtrate water is a representation of the *real* pore solution obtained through for example PSE. This is a fast, cheap and simple method, but it has some drawbacks, as dilution and carbonation during the measurements can cause deviations [5]. Ex-situ leaching is referred to as cold water extraction (CWE), and is done in four steps; powdering of samples, leaching, filtration and analysis, as shown in Figure 8
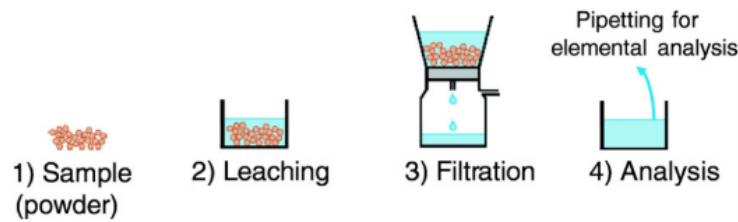
Figure 8: Cold water extraction procedure. From [25]

Plusquellec et al. [25] concludes that PSE is a reliable method for obtaining pore solution and for determining the pH. Their findings show a lower pH in CEM II/B-V than for CEM I after 28 days curing. They state that the difference in pH most likely comes from the dilution of cement and the subsequent pozzolanic reaction of fly ash. Table 3 show the pore solution composition of the samples made by Plusquellec et al. They also conclude that CWE is not suitable for determining pH, as dilution of alkali metal ions will lead to a decrease in the pH. It is though recommended to use CWE in the determination of the free alkali metal content, and to calculate the pH on the basis of the elemental composition [25].

Table 3: Composition of extracted pore solution measured by ICP-MS after performing pore solution expression on non carbonated mortar samples. Table recreated from Plusquellec et al. [25]. Numbers in mmol/l.

	Na		K		Ca		Al		Si		S	
	Average	Std dev	Average	Std dev	Average	Std dev	Average	Std dev	Average	Std dev	Average	Std dev
CEM I	263.8	2.6	380.9	5.9	1.4	0.04	0.2	0.02	0.5	0.03	11.1	0.4
CEM II/B-V	143.2	–	208.6	–	1.5	–	0.46	–	0.6	–	4.3	–

The drawback of the PSE method is that it requires sufficient moisture in the sample in order

to extract enough pore solution. The ex-situ leaching technique does not require moist samples,and can be performed on dry samples.

Qi Pu et al. (2012) [28] investigated the pH and the chemical composition change in pore solution upon carbonation of OPC and fly ash. They used 3 mm thin discs exposed to 40 % RH and 5 % CO_2 to ensure fast carbonation. They found that the alkali content in carbonated material was only 20 - 40 % of the non-carbonated alkali content as shown in Figure 9.
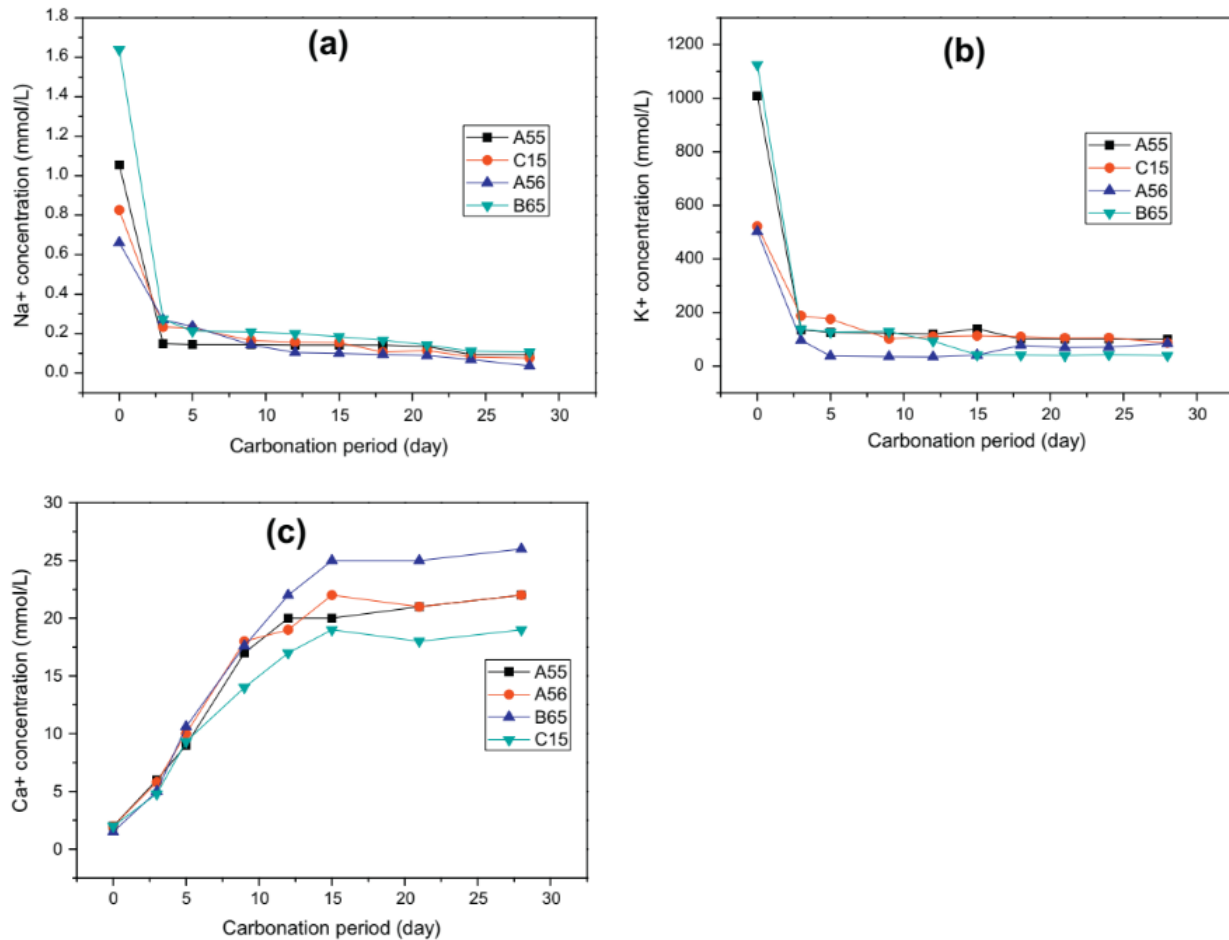
Figure 9: Sodium, Potassium and Calcium content in the pore solution of different concretes. A - OPC cement (500 kg/m^3), B - OPC cement (600 kg/m^3), C15 - fly ash blended cement (425 kg/m^3 cement, 75 kg/m^3 fly ash). Graphs from [28].

De Weerdt et al. (2011) [10] investigated the difference in the pore solution composition of cement pastes made with Portland cement (OPC) fly ash blended Portland cement (OPC-FA). They found that for OPC, the Na and K concentration and the pH increase over time. For OPC-FA, the alkali concentrations are lower than for OPC, and that the alkali concentration is decreasing after 28 days of curing. They state that the reason for this is the incorporation of alkalies in the

hydration products formed by the fly ash. They also show that replacing OPC with fly ash lowers the sulphate concentrations.

2.5   Carbonation Detection

Carbonated concrete has a lower pH than non carbonated concrete. One of the most common ways to determine the carbonation front in concrete structures is to open the sample and spraying it with phenolphthalein or thymolphthalein. These are pH indicator liquids that change colour in pH around 8-10. In pH above 10 it has a color, below it is colorless. Carbonated concrete is known to have a pH below 9, whereas non carbonated concrete often has a pH in the range of 13. Figure 10 shows a sample that is cut open and sprayed with thymolphthalein. The carbonation front is clearly visible.
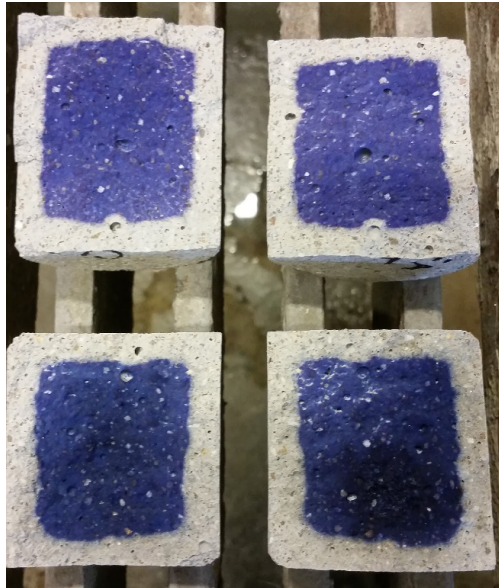
Figure 10: Sample sprayed with thymolphthalein. Sample cured for 3 days, exposed to 60 % RH and 1 % CO_2 for 2 weeks.

2.6   TGA-analysis

Thermogravimetric analysis (TGA) is often used as a method for quantifying the phases in concrete [7]. The principle of the method is to heat a sample from room temperature to 900^oC and measuring the weight loss in the sample continuously. As the sample is heated, the release of H_2O and CO_2 is measured in the form of weight loss. The free water is lost (evaporated) at 100 ^oC, whereas chemically bound water is released at much higher temperatures. The amount of energy (or the temperature) required to split a phase is different for different phases, and the

amount of each phase can then be determined with TGA. For example, calcium hydroxide re-leases water at around 400 - 500 ^{o}C, whereas calcium carbonate releases CO_2 at around 500 - 800 ^{o}C. During carbonation, CO_2 reacts with calcium hydroxides, among other elements, so a TGA analysis of a carbonated material should show no amount of calcium hydroxide.

3 Experimental

In this chapter the materials used, casting, curing, exposure, preparation of the samples and tests performed are described.

3.1 Overview

An overview of all the tests performed and the parameters investigated is shown in Table 4. All the tests are described further in this chapter.

The notation used further in this thesis is for example CEM II/B-V 90-5 and CEM I 60-1. The notation "90-5" means that the sample is stored at 90 % RH and 5 % CO_2-concentration. The samples stored in desiccators is notated 90-0 and 60-0.

Table 4: Overview of parameters investigated and tests performed in this thesis.

Cement	Condition	Resistivity testing	Corrosion potential testing	Pore solution extraction technique	Pore solution analysis	Carbonation investigation	Pore structure testing
CEM I	60-0	Y	Y	CWE	ICP-MS	TGA	PF
	60-1	Y	Y	CWE	ICP-MS	TGA	PF
	90-0	Y	Y	CWE	ICP-MS	TGA	PF
	90-5	Y	Y	CWE*	ICP-MS*	TGA	PF
	Sealed	N	N	PSE + CWE	ICP-MS	-	PF
CEM II/B-V	60-0	Y	Y	CWE	ICP-MS	TGA	PF
	60-1	Y	Y	CWE	ICP-MS	TGA	PF
	90-0	Y	Y	CWE	ICP-MS	TGA	PF
	90-5	Y	Y	CWE*	ICP-MS*	TGA	PF
	Sealed	N	N	PSE + CWE	ICP-MS	-	PF

*CWE and ICP-MS analysis performed on samples crushed and exposed for 8 more weeks. As a consequence, these results are not comparable to other results of the same sort.

Plastic bottles were used as moulds in order to prevent early drying of the samples during hydration. Also, the diameter of the bottles made it possible to perform the pore solution expression test without adjusting the geometry of the sample.

The amount, type and cement type of each bottle casted is shown in Table 5.

Table 5: Number and types of bottles and cement type for all batches. I = CEM I, II = CEM II/B-V

Batch	1	2	3	4	5	6	7	8	9	10	11	12
Cement type	II	II	II	II	I	I	I	I	II	II	I	I
Plain	5	5	5	5	5	5	5	5	7	7	7	7
Instrumented	1	1	1	1	1	1	1	1	-	-	-	-
Reinforced	1	1	1	1	1	1	1	1	-	-	-	-

As presented in the table, there are 5 plain, 1 instrumented and 1 reinforced bottles per batch. Each bottle were sawn into three 15 mm discs, hereafter referred to as samples. The layout of the different samples are shown in Figure 11. The samples with embedded materials were dedicated to specific tests, whereas the plain samples could be used more freely.

(a) Reinforced bottle and sample for corrosion potential testing.

(b) Instrumented bottle and sample for resistivity testing.

(c) Plain bottle and sample for pore solution extraction and PF-testing.
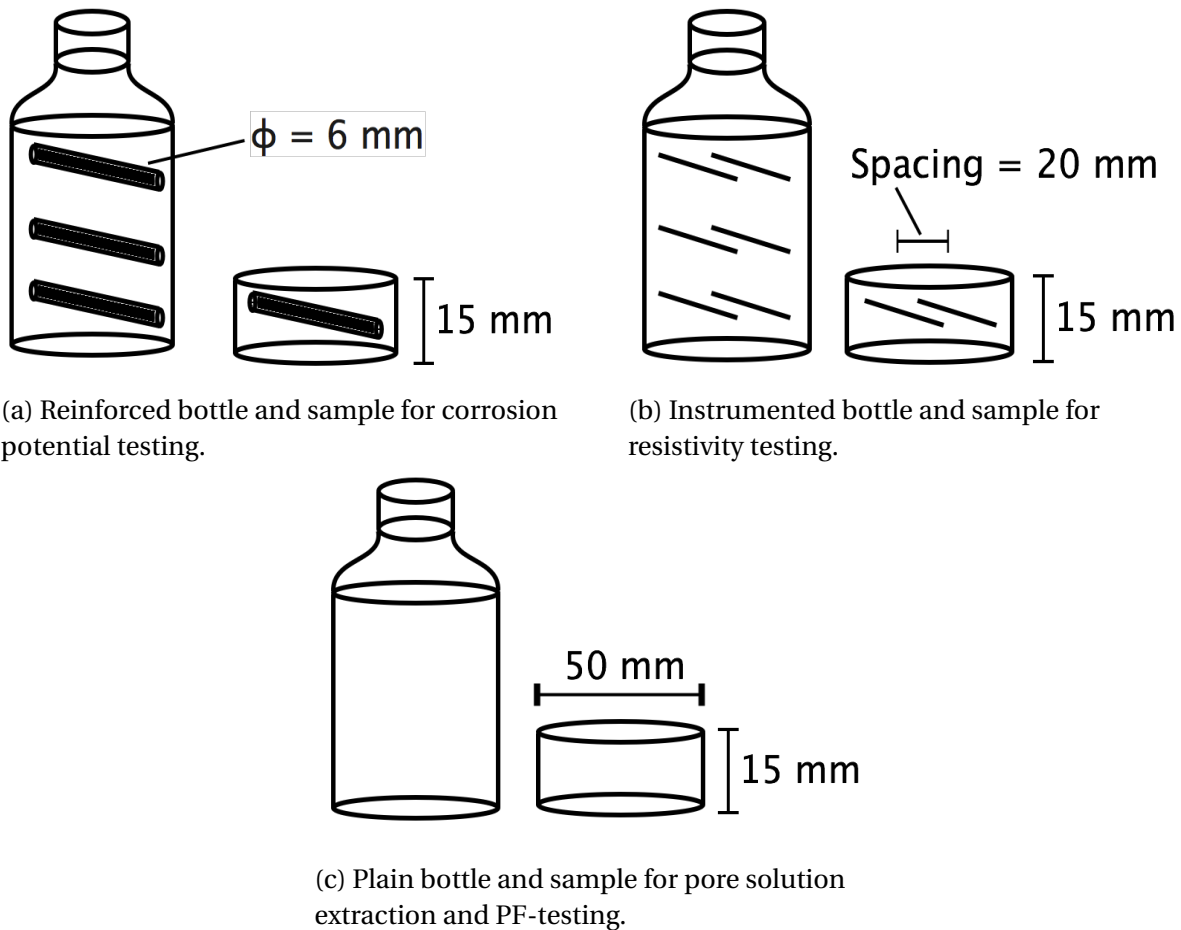
Figure 11: The different types of casted bottles and the samples they were sawn into.

3.2 Materials

Two cements were used and compared in this project. CEM I and CEM II/B-V. The chemical composition of each cement is shown in Table 6.

Table 6: Chemical composition of the cements used. All numbers in % of weight. Data from [22]

	SO_3	SiO_2	Al_2O_3	Fe_2O_3	CaO	MgO	P_2O_5	K_2O	Na_2O	Alkali
CEM I	3.48	20.44	4.77	3.43	61.71	2.19	0.17	0.92	0.51	1.12
CEM II/B-V	3.16	29.52	10.76	4.51	44.63	2.01	0.39	1.06	0.47	1.17

The sand used is of the type CEN-Standard Sand EN 196-1. Grain size distribution is shown in Table 7. The sand was delivered in bags of 1350 ± 2 grams, with a maximum moisture content of 0.2 % [23].

Table 7: Grain size distribution. Data from [23]

Mash size [mm]	Lower limit [%]	Intervall average [%]	Upper limit [%]
2	0	0	0
1.6	2	7	12
1	28	33	38
0.5	62	67	72
0.16	82	87	92
0.08	98	99	100

The reinforcement used was carbon steel B500NC with a diameter of 8 mm. The composition of the steel is shown in Table 8.

Table 8: Chemical composition of B500NC [%] according to NS 3576 (NS-3576-3, 2012)

Element	C	Si	Mn	P	S	N	Cu
% of mass	0.24	0.65	1.7	0.055	0.055	0.014	0.85

For the resistivity testing, titanium rods with diameter 2 mm were embedded in the samples. The composition of the titanium bars used is shown in Table 9.

Table 9: Chemical composition of titanium bars. Data from [1]

Element	N	C	H	Fe	O	Al	V	Ti
% of mass	0.015	0.01	0.005	0.095	0.05	/	/	Balance

The mortars were made with a water to cement ratio of 0.55. The theoretical and real matrix is shown in Table 10 and 11

Table 10: Theoretical matrix design

	Materials		
Cement type	Cement	Water	Sand
CEM I	424.8	233.7	1350
CEM II/B-V	424.8	233.7	1350

Table 11: Real (measured) matrix composition

		Materials		
Batch	Cement type	Cement	Water	Sand
1	CEM II/B-V	424.9	233.4	1345.1
2	CEM II/B-V	424.6	233.8	1348.7
3	CEM II/B-V	424.6	233.2	1347.8
4	CEM II/B-V	424.6	233.9	1348.1
5	CEM I	424.8	233.9	1350.1
6	CEM I	424.6	233.5	1349
7	CEM I	424.7	233.9	1349.9
8	CEM I	424.7	233.7	1351.2
9	CEM II/B-V	424.7	233.6	1345.3
10	CEM II/B-V	424.4	233.4	1347.9
11	CEM I	424.7	233.6	1351.4
12	CEM I	424.6	233.4	1349.8

3.3 Casting

Before the main casting in this thesis, a small test-casting was performed to ensure the procedure for compaction resulted in homogeneous samples. The samples were compacted using

jolting and vibration. The samples were then cured for 3 days in climate cabinet, before they were exposed to 60 % RH and 1 % CO_2 for 3 weeks. The samples were then split and the carbonation front was investigated using thymolphthalein. The carbonation front shown in Figure 12 indicate that both compaction methods provide homogeneous samples.
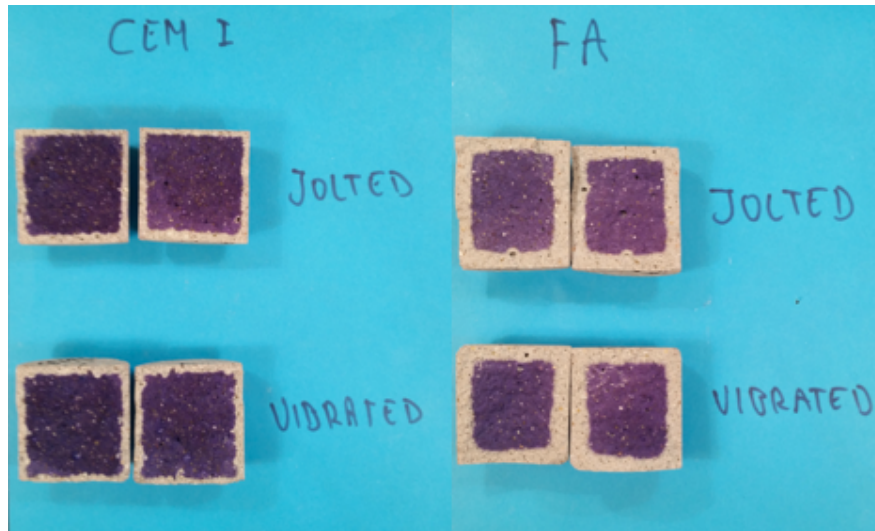
Figure 12: Samples from the test-casting sprayed with thymolphthalein to investigate the carbonation front after 3 days of sealed curing and 3 weeks of exposure to 60 % RH and 1 % CO_2.

The main casting was done 10.05.2017.

In total 12 batches of mortar were casted, resulting in 84 regular and 8 small bottles. Each bottle was filled in three layers, approximately 1/3 of the height of the bottle. Each layer were compacted by jolting 30 times.

The casting procedure is done with a mixer as shown in Figure 13 according to EN-196. The casting procedure was done this way:

- The bowl is cleaned with a wet cloth

- Water is added

- Cement is added

- The mixer is started on low speed immediately after the water and the cement is placed in the bowl

- After 30 seconds of mixing, sand is steadily added for the next 30 seconds

- The mixer is set to high speed for 30 seconds

- Mixing is stopped for 90 seconds and mortar adhered to the wall and bottom of the bowl is manually scraped off and placed in the middle of the bowl

- Mixing is continued for 60 seconds at high speed

The process of mixing one batch took 4 minutes, and contained enough mortar for 7 regular and 1 small bottle.

Figure 13: The cement mixer used.

3.4 Curing

After casting the bottles were placed in a tray. The bottom of the tray was filled with water and the whole tray was wrapped in plastic to ensure 100 % relative humidity. The bottles were then stored in a climate cabinet at 20^oC for 14 days.

3.5 Exposure

For carbonating samples: Two different environment were chosen for the carbonating samples. One with 1 % CO_2 and 60 % RH, another with 5 % CO_2 and 90 % RH. The samples are shown in Figure 14. Table 12 show the environments and where the batches are placed after curing.

Figure 14: Bottles sawn into discs, placed in carbonation cabinet.

Table 12: Exposure environments and sample placement.

RH [%]	90	90	60	60
CO_2 [%]	0	5	0	1
Plain	5	5	5	5
Instrumented	1	1	1	1
Reinforced	1	1	1	1
Batch	1 and 5	2 and 6	3 and 7	4 and 8

For non-carbonating samples: In order to have references for the carbonating samples, each set of carbonating samples had a corresponding set of non-carbonated samples. These were kept in the same relative humidity, but without the presence of CO_2. This means two environments with 0 % CO_2, one with 60 % RH and one with 90 % RH. Relative humidity of 60 and 90 was achieved by placing the samples in desiccators over saturated salt solutions of sodium bromide (NaBr) and barium chloride ($BaCl_2 \cdot 2\,H_2O$), respectfully [18][19]. Figure 15 show the desiccators.
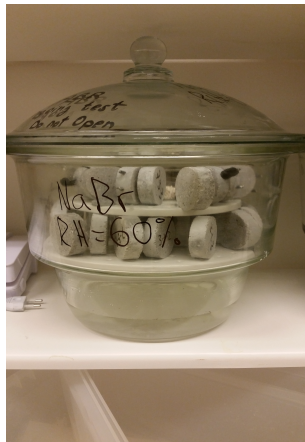
(a) Desiccator for 60 % RH.

(b) Desiccator for 90 % RH.

Figure 15: The two desiccators used.

3.6 Method - the samples, pretreatment and tests

Most of the samples are dedicated to one specific test. In the sections below the samples and how they were treated, from preparing to testing, are described.

Table 12 show the different exposure conditions and where the batches were placed.

This means all the bottles from batch 1-8 has been "assigned" to a specific test. The remaining

bottles (7 made with CEM I and 8 made with CEM II/B-V) was kept sealed in a climate chamber at 100 % RH and 20°C.

3.7   General

All the samples specified for a test were sawed into discs with a height of 15 mm. This was done in order to achieve full carbonation in the time available. In order to estimate the time for full carbonation, a simple calculation with base in a existing carbonating sample was made. A sample of CEM I was exposed for 31 weeks with 5 % CO_2 in 90 % RH and had a carbonation front of 10.2 mm. Converting this into a two-sided exposure, the 15 mm discs was estimated to be fully carbonated after 17 weeks after exposure.

All the discs were labeled with three numbers: the first is for batch number, the second for bottle number, and the third is for disc number (1 is bottom, 3 is top). So, the top disc of bottle number 4 from batch 2, will be labeled 2-4-3.

3.8   Concrete resistivity

In total 8 bottles (24 discs). Titanium-rods were placed in the samples to test the resistivity of the mortars. The bottles were cured as described and sawed into 3 discs, each disc containing 2 rods. The rods were placed horizontally in the bottle, with 20 mm between them. The titanium rods were covered in shrinking plastic, leaving 20 mm of uncovered titanium inside the sample. After mounting the rods, the joint between bottle and rod were sealed with glue to prevent leaking during casting as shown in figure 16.

Figure 16: Bottle with embedded titanium rods for resistivity testing

The test was done as a two-electrode system shown in Figure 1b), where clamps were fastened on the two titanium rods to ensure a proper electrical connection. AC current was applied using

an LCR meter (frequency ranging from 0.10 kHz to 10 kHz, square pulse ca. 0.9 V). The frequency was adjusted between 0.1 and 10 kHz to find the lowest phase angle for each sample.

As shown in Equation 1, a cell constant (k) must be determined in order to calculate the resistivity of a sample. When this value is determined, resistivity can be calculated by just measuring the resistance of the mortar disc. This constant was estimated with tap water in the bottles, taking three measurements with different water-heights. First the tap water resistance was measured in a known volume (thereby a known cell constant), giving the resistivity of the water as shown in Table 13.

Table 13: Estimating the resistivity of tap water. The frequency was set to 1 kHz. The cell constant is in this case the area divided by the length. Equation 1 gives the resistance.

	A	0,01	m^2			
Tap water	L	0,1	m	ρ	89,9	Ω·m
	R	899	Ω			

The bottom pair of rods were measured with a water-level approximately 1/3 of the bottle. The middle pair with water level 2/3, and the top pair with water in the whole bottle. When using AC current, it is important to use the frequency that gives the lowest phase angle (θ). This is shown in Table 14 together with the test results.

Table 14: Measurements of resistance in bottles filled with tap water. Arrangement 1 = bottom pair of rods. The cell constant is calculated from Equation 1. Applied frequency was 1 kHz.

Batch/ bottle	Arrangement - R [kΩ]			θ []			Cell constant [m]		
	1	2	3	1	2	3	1	2	3
1	4	4	3.71	-0.4	-0.4	-0.3	0.022	0.022	0.024
2	3.9	3.9	3.81	-0.3	-0.3	-0.3	0.023	0.023	0.024
3	3.9	3.9	3.65	-0.4	-0.4	-0.3	0.023	0.023	0.025
4	4.3	3.7	3.6	-0.4	-0.4	0.4	0.021	0.024	0.025
5	3.9	3.74	3.52	-0.4	-0.4	-0.4	0.023	0.024	0.026
6	4	3.7	3.67	-0.5	-0.5	-0.4	0.022	0.024	0.024
7	3.92	3.7	3.79	-0.4	-0.4	-0.7	0.023	0.024	0.024
8	3.65	3.42	3.46	-0.4	-0.4	-0.4	0.025	0.026	0.026

The cell constant is plotted in Figure 17, and shows that the cell constants are pretty similar. It is therefore possible to use the same value for all the samples, k=0.0238.
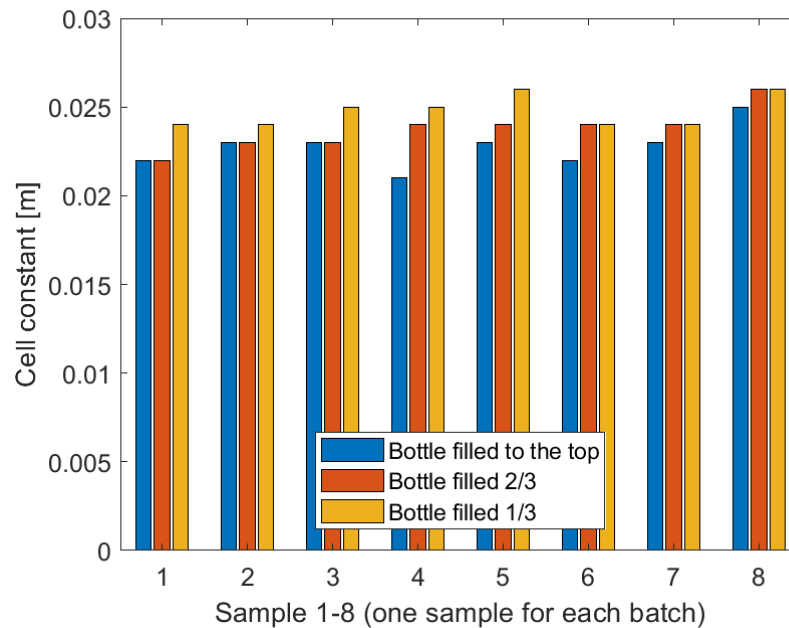
Figure 17: Cell constants plotted in a diagram. Values from Table 14.
Mean cell constant value = 0.0238.

Resistance measurements was taken every week from 18 to 28 weeks of exposure and plotted in Figure 23 and 24. The measurements in full is shown in Appendix A.4

3.9 Pore structure testing

8 bottles were casted for the PF-test. The bottles were cured as described for 14 days and sawed into 3 discs, each with thickness 15 mm. Each disc was tested individually. Both carbonated, non-carbonated and sealed samples was tested.

The PF test determines the suction porosity and the macro porosity as well as the degree of capillary saturation by weighing the sample under different conditions [12]. The test performed here is a modified version of the PF-test described in Statens Vegvesens "Investigation of concrete from Solsvik field station (2015) [12].

1. Weigh the sample on a balance with accuracy 0.001 g (W_1)

2. Dry the specimen at 105^oC until constant mass (mass change over half a day <0.01%). Dry weight is measured (W_2)

3. The samples are placed in a water bath, partly submerged the first day (one surface over the water, fully submerged after first day), until stable mass after which they were weighted

in air (W_3) and under water for volume determination (W_4=V)

4. Finally the samples were dried at 105^oC until constant mass and weighted in air (W_5)

The procedure for weighing:

- Take the samples out of the oven

- Put the samples in a desiccator to let them cool down without the influence of moisture (this normally takes 1-2 hours)

- Weigh the samples on a balance with accuracy 0.001 g

- Put the samples back in the oven

The following formulas are used for calculating volume, water content, degree of capillary saturation and suction porosity:

$$Volume\ (V) \ = \ W_3 - W_4 \ [cm^3]$$

$$Water\ content \ = \ \frac{W_1 - W2}{W1} \cdot 100\% \ [weight\%]$$

$$Degree\ of\ capillary\ saturation\ (DCS) \ = \ \frac{W_1 - W_2}{W_3 - W_2} \cdot 100\% \ [\%]$$

$$Suction\ porosity\ (pore\ volume) \ = \ \frac{W_3 - W2}{V} \cdot 100\% \ [volume\%]$$

Comparing W_5 and W_2 to see if the sample has been destroyed by the drying/saturation cycle.

The samples were weighted and put in the oven at 105^oC 01.11.2017. The samples was dried for 16 days. The samples were then placed in a water bath on 17.11.2017. This was a Friday, and until Monday the samples were partly submerged, meaning that one face of the sample were not under water. After the partly submerged period, the samples were fully submerged. The samples was weighted under water and dry until stable weight was obtained.

When checking the weight after 3 days in the cabinet, the first weighting were done immediately after removing the samples from the oven (when they were cold enough to touch) and then another weighing after they had cooled down to room temperature (roughly 3 hours). The "cold weighing" showed an increase in weight of about 0.02 - 0.07 %. This means that the "hot weight" was showing a weight with great error, especially when considering that the criteria for stable weight is only 0.01 g/half day. The hot air surrounding the sample could create an uplift,

resulting in the weight showing a lighter sample. After seeing this, the rest of the weightings were done on cold samples.

3.10 Potential measurements

In total 8 bottles (24 discs) were casted for this test. The samples were cured as described and sawed into 3 discs, each disc containing one bar of reinforcement. The reinforcement used has a diameter of 8 mm, resulting in 3.5 mm cover in each disc. All reinforcement bars were covered in shrinking plastic, leaving 30 mm of uncovered area inside the sample. The reinforcement and the corresponding bottle is shown in Figure 18. After placing the reinforcement in the bottle, the joints between reinforcement bar and bottle were sealed with glue to prevent moisture from coming in contact with the steel, and to prevent leaking of mortar during casting.

Before mounting the reinforcement bars in the bottles, all the bars were weighted. The weight of each bar used and their placement in the samples are shown in Table 19 in Appendix A.2. It will not be done in this project, but the samples can be opened and the reinforcement bars weighted against their initial weight to investigate the corrosion.

When the samples was carbonated, potential measurements was performed. This was done with a reference electrode (SCE) placed on top of the disc, and a wire connected to the reinforcement. This was connected to a high impedance voltmeter (Fluke 76, input impedance 10 M Ω), as shown in Figure 19.

Figure 18: Reinforcement bars and bottle before mounting

Figure 19: Setup of corrosion potential measurement.

Potential measurements were taken every week from 18 to 28 weeks of exposure on both carbonated and not carbonated samples.

3.11   Pore solution investigation

Two different tests were performed for this purpose, pore solution extraction (PSE) and cold water extraction (CWE). Originally, only PSE were to be performed, but after exposure the samples appeared to dry to yield any pore solution through PSE. Therefore, CWE was introduced for the exposed samples, and PSE was performed on the sealed samples. To compare the methods, sealed samples were also included in the CWE.

3.11.1   Pore solution expression (PSE):

The pore solution expression test is basically squeezing the pore water out of a sample under pressure. The machine used is shown in Figure 20a. In principle, a sample is placed in a hollow steel cylinder and then placed under a steel piston that applies hydraulic pressure to the sample [5]. The cylinder is placed on a base plate with drainage channels, leading the pore solution out through a small tube and into a syringe as shown in Figure 20b. The test procedure is as follows:

- The sample is placed in the cylinder with a Teflon disc between the sample and the piston

- The piston is lowered onto the sample

- The pressure is slowly increased to 30 tons (150 Mpa)

- 30 tons is applied for 10 minutes

- After 10 minutes, the pressure is increased steadily up to 55 tons (275 MPa) or until the sample has provided enough solution

- 55 tons is maximum pressure used, and it can be applied until enough pore water is obtained, or for 1 - 2 hours

(a) The machine used for pore solution extraction.

(b) Setup for pore solution extraction.

Figure 20: Pore solution extraction machine and setup.

After squeezing the sample, the pore solution was diluted and acidified the same way as the filtrate obtained from CWE, according to [26].

The samples casted in the test-casting were put through PSE after 3 weeks of exposure and yielded no pore solution.

3.11.2 Cold water extraction (CWE):

Cold water extraction was in three steps. First, the samples was grinded in a powder mill. The powder was then mixed with deionized water and filtrated. The solution was then diluted and acidified as described by Plusquellec and De Weerdt (2017) [26].

Procedure for powdering of samples:

- Crush the sample into pieces <10 mm with a jaw crusher. Collect the pieces and place them in a plastic bag and store in a desiccator over soda lime

- Put the crushed material in the powder mill

- Seal and close the mill

- Select the program "1500 rpm - 30 secs" and launch it

- Scratch the grinding elements with a spatula to recover most of the powder

- Put the powder in plastic bags, seal and label the bags

- Place the bags in desiccator containing soda lime

- Clean and dry all used equipment before grinding another sample. Sand (Normensand) and water grinded for 30 seconds will remove most of the powder. A metallic sponge is used to clean the grinding elements of the mill

Procedure for leaching and filtration:

- Prepare and install the filtration unit

- Weigh carefully and precisely 20.000 g of the powdered sample using a spatula in a beaker. Write down the mass

- Weigh carefully and precisely 20.000 g of the freshly deionized water in a second beaker. a Pasteur pipette is used at the end to obtain small drops and be precise enough. Write down the mass

- The magnet is put in the beaker containing the powder, which is placed on the magnetic stirrer

- Put the magnetic stirrer on at a low speed, i.e. 1. The heating mode has to be turned off

- Add slowly the deionized water and start the timer. Adjust the speed of the stirrer: high enough to ensure good mixing, but splashing must be avoided. The mixing can be helped by carefully moving the beaker on the stirrer

- When the 5 mins are over, the suspension is immediately filtered using the filter device

- When all the solution has passed through the filter, it is poured from the Erlenmeyer into a 15 ml centrifuge tube properly labelled. The remaining filtrate is discarded

Procedure for dilution and acidification:

- The nitric acid HNO_3 has to be first diluted by 2 with deionized water. Then performing the dilution, remember to always measure the deionized water first, and then add the acid to the water.

- Pipette 1 ml of the filtrate in the centrifuge tube

- Pipette 9 ml of deionized water in the same tube

- For a diluted sample of 10 ml, 0.140 ml of the diluted HNO_3 has to be added in order to obtain 0.1 mol/l of HNO_3 in the sample. It has to be kept in mind that the addition of acid

induces a dilution which has to be taken into account. For example, the acidification of a 10 times diluted solution will increase the dilution factor to 10.14

- All tubes has to be properly labelled (sample name, date, dilution, acidification etc.)

3.11.3 ICP-MS

After performing CWE, the pore solution obtained was sent to Department of Chemistry, NTNU, for Inductively Coupled Plasma Mass Spectrometry (ICP-MS) analysis. Syverin Lierhagen was responsible for performing the analysis. Through ICP-MS the pore solution composition was determined. Based on the results obtained by ICP-MS, the content of elements of the sample was calculated as the following:

$$x[mol/g_{mortar}] = \frac{[x]_{measured} \cdot D}{M(x)} \cdot \frac{m_{water}}{m_{powder}} \cdot 10^{-9} \tag{2}$$

where x is measured element, i.e. Na, K and so on, $[x]_{measured}$ is the concentration of element x (in μg/l) measured by ICP-MS, D is the dilution factor, M(x) is the molar mass of element x, m_{water} is the mass of deionized water added to the powder during CWE and m_{powder} is the mass of powdered material used.

In order to calculate back to mol/l in the solution obtained through CWE, the following formula was used:

$$x[mol/l] = \frac{[x]_{measured} \cdot D}{M(x)} \cdot \frac{m_{wateradded} + m_{powder} \cdot \%m_{freewater}/100}{m_{powder} \cdot \%m_{freewater}/100} \cdot 10^{-6} \tag{3}$$

where x is measured element, $[x]_{measured}$ is the concentration of element x (in μg/l) measured by ICP-MS, D is the dilution factor, M(x) is the molar mass of element x, $m_{wateradded}$ is the mass of deionized water added to the powder during CWE, m_{powder} is the mass of powdered material used and $m_{freewater}$ is the amount of free water in the material (see Figure 25a).

The pore solution obtained through PSE was also sent for ICP-MS analysis. The formula used to calculate back to mol/l was the following:

$$x[mol/l] = \frac{[x]_{measured} \cdot D}{M(x)} \cdot 10^{-6} \tag{4}$$

where x is measured element, $[x]_{measured}$ is the concentration of element x (in μg/l) measured by ICP-MS, D is the dilution factor and M(x) is the molar mass of element x.

All formulas are obtained from [26].

3.12 Carbonation detection

To determine the degree of carbonation in the samples, thymolphthalein was used. This is a pH indicator that changes color in the pH range of 9 to 10.5. Below this range thymolphthalein appear colorless, and above this range it shows a strong blue color. The thymolphthalein solution was prepared by dissolving 1 g of the indicator in a mix of 30 ml of deionized water and 70 ml of ethanol. Thymolphthalein was sprayed on the freshly split samples to investigate the degree of carbonation.

3.13 TGA

Thermogravimetric analysis (TGA) was performed on different samples in order to confirm the degree of carbonation. Since the samples in 90-5 carbonated at a slower rate than first assumed, these samples were split in smaller pieces to speed up the carbonation process. Before putting the samples through the CWE and ICP-MS analysis, the samples were analyzed with TGA to confirm full carbonation. For reference, samples from 60-1 and 60-0 were also put through the TGA process. The TGA curves from 90-5 and 90-0 were then compared to the curves obtained from 60-1 and 60-0. The results are shown in the results chapter.

TGA was performed with a Mettler Toledo TGA/DSC 3+, on samples of approximately 300 mg loaded in aluminum oxide crucibles. The samples were heated from 40^oC to 900^oC at a rate of 20^oC/min while the oven was purged with N_2 at 50 ml/min. The weight loss of the samples was monitored as a function of the temperature.

The TGA graph was exported to a .txt file, and all the data points was plotted in MATLAB to obtain the graph shown in Chapter 4. The amount of $Ca(OH)_2$ and $CaCO_3$ was calculated by horizontal step from the graph, and is shown in a bar chart. From the graph given by the "TGA-machine" the amount of CH and CC̲ is given in mg, but this weight is the amount of evaporated water. This is because the TGA measures a change in weight, and all the weight change is caused by the evaporation of water and the release of CO_2. The two reactions that is happening are:

CH: $Ca(OH)_2$ –> $CaO + H_2O$

CC̲: $CaCO_3$ –> $CaO + CO_2$
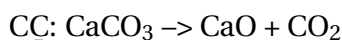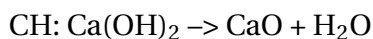
Mol-weights:

- $Ca(OH)_2$ - 74 g/mol

- H_2O - 18 g/mol

- $CaCO_3$ - 100 g/mol

- CO_2 - 44 g/mol

In order to calculate back to CH and CC in weight % of the sample, these formulas are used:

$$m_{dry} = m_{40^oC} - m_{800^oC} \tag{5}$$

$$m_{CH}[weight\%] = \frac{m_{CH}[mg]}{m_{dry}} \cdot \frac{74}{18} \cdot 100\% \tag{6}$$

$$m_{CC}[weight\%] = \frac{m_{CC}[mg]}{m_{dry}} \cdot \frac{100}{44} \cdot 100\% \tag{7}$$

4 Results

Resistivity and corrosion potential measurements have been performed through several weeks, shown in Figure 23, 24, 27 and 28. Pore structure investigation, CWE, ICP-MS, PSE and TGA was performed after 27 weeks of exposure, and are shown in Figure 25, 29, 30, 21 and 22. CWE and PSE was performed on sealed samples and compared, shown in Figure 31 and 32.

4.1 TGA

Figure 21 and 22 shows results from TGA. TGA was performed 24.11.2017 - 07.12.2017. The results from 60-0, 60-1 and 90-0 can be compared with results from pore structure investigation, resistivity and ICP-MS, as these samples were whole when the TGA was performed. For 90-5, the samples were crushed and exposed for 9 weeks before TGA was performed, and are therefore not comparable to the other tests done, as the degree of carbonation is not equal for the other tests.

Each line in Figure 21 represents one sample. TGA was performed on the middle disc of one bottle from each batch casted (described in Chapter 3).

Figure 21 show the weight loss recorded by TGA and the differential thermogravimetry (DTG) data. The peak at 400 - 500 ^{o}C show the amount of calcium hydroxide (CH) in the samples, while the peak between 500 - 800 ^{o}C show the amount of calcium carbonates (C$\underline{C}$) presented as weight loss of water and carbon dioxide, respectively. Samples from desiccators show a large amount of CH, while samples from 60-1 and CEM II/B-V from 90-5 show no amount of CH. CEM I, 90-5 show a small amount of CH and a larger amount of C$\underline{C}$, as shown in Figure 22.

Figure 22 show the amount of CH and C$\underline{C}$ in the samples, calculated as described in Chapter 3. Both samples (CEM I and CEM II/B-V) from 60-1 show no amount of CH, while the opposite is seen in samples from 90-0 and 60-0. CEM II/B-V, 90-5 show no amount of CH and a large amount of C$\underline{C}$, while CEM I, 90-5 show a small amount of CH (also seen in the peak in Figure 21) and a larger amount of C$\underline{C}$.
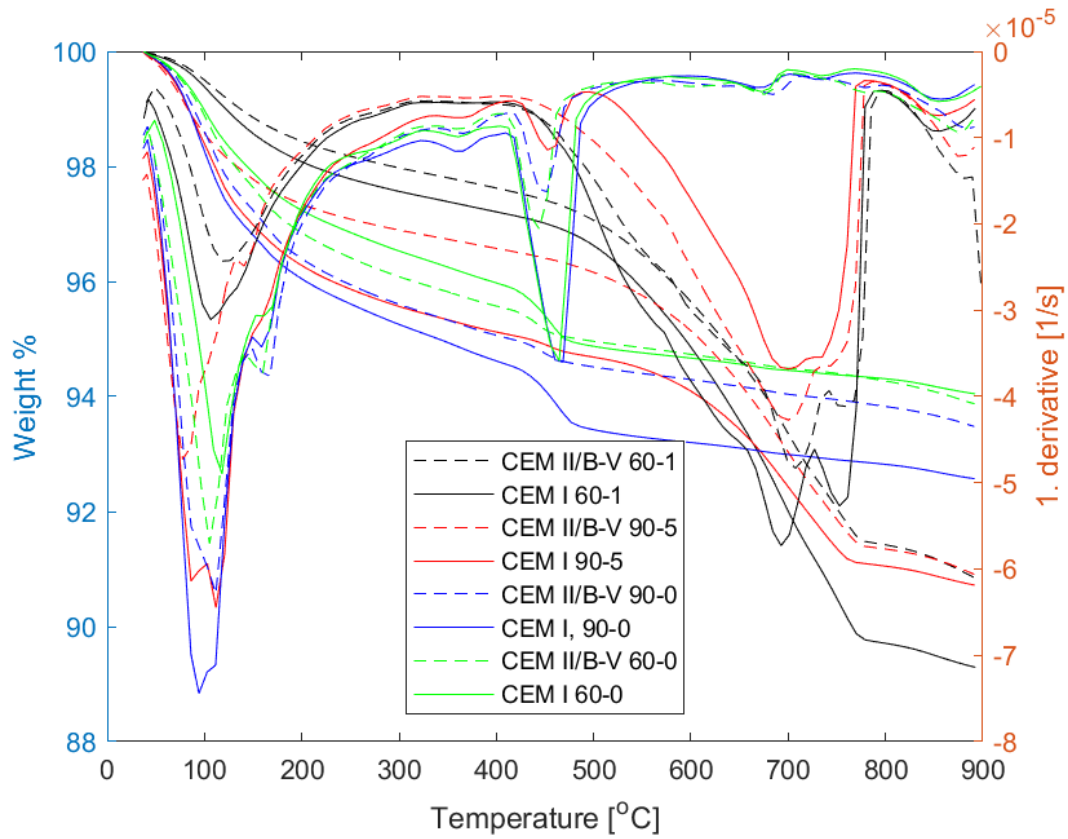
Figure 21: Weight loss of samples obtained from TGA analysis after 2 weeks of sealed curing and 27 weeks of exposure. The samples from 90-5 were crushed 8 weeks prior to analysis.
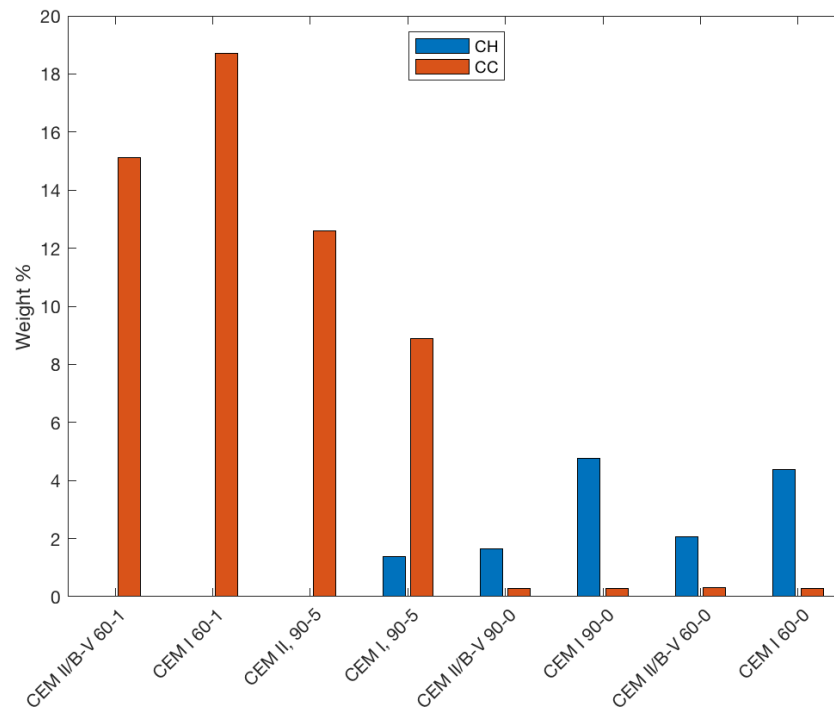
Figure 22: Content of Ca(OH)$_2$ (CH) and CaCO$_3$ (CC) obtained from TGA analysis after 2 weeks of sealed curing and 27 weeks of exposure. The samples from 90-5 were crushed 8 weeks prior to analysis

4.2   Resistivity

Resistance measurements were taken weekly until 28 weeks of exposure. The resistivity was then calculated using Equation 1. The full set of measurements is shown in Appendix A.4. The measurements were then stopped, as the other tests were taken at 27 weeks of exposure, and further results were not comparable with the other results. The measurements were taken as described in Chapter 4.6 - Method. Figure 23 show resistivity values for samples in exposure conditions 60-0, 90-0 and 90-5. Figure 24 show resistivity values for samples in exposure condition 60-1. The results were plotted in two separate graphs as the results from 60-1 were considerably higher than the other samples.

Figure 23 and 24 show one line with error bars per cement per exposure condition. Each line represents the average value of three samples, and the error bars represents the lowest and highest resistivity value for the three samples. The resistance measurements were taken in kΩ with a accuracy of 0.01 kΩ. The full set of measurements are shown in Appendix A.4.

As seen in Figure 24, samples from 60-1 show the highest resistivity, with values ranging from 30

000 to 70 000 Ωm. Samples from 90-0, 90-5 and 60-0 is presented in Figure 23. CEM II/B-V show the highest resistivity for this group, while all the CEM I samples show resistivity of 500 Ωm and lower.
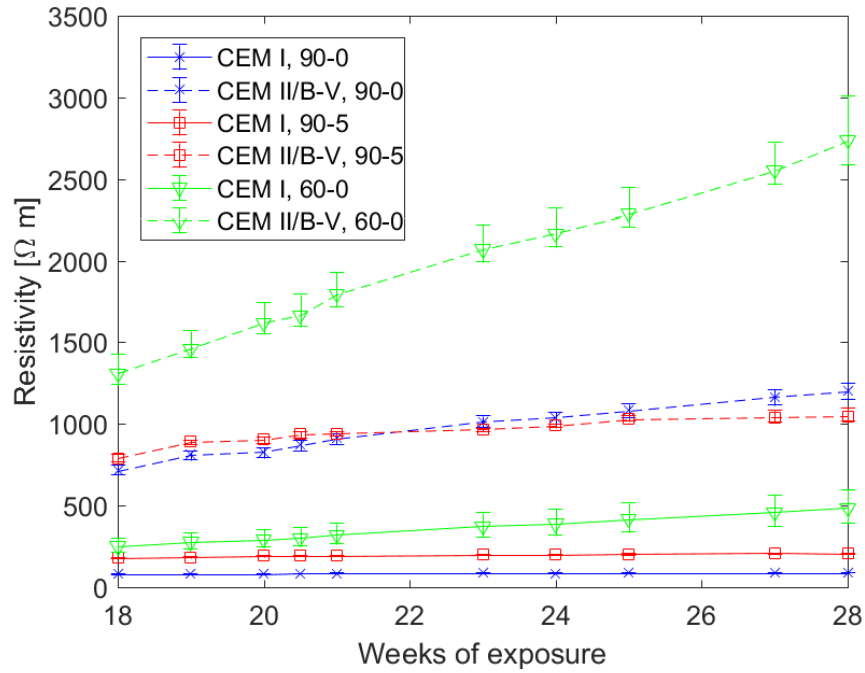
Figure 23: Resistivity of samples in different exposure conditions. The samples were cured for 2 weeks before exposure. Each line is average value of 3 samples.
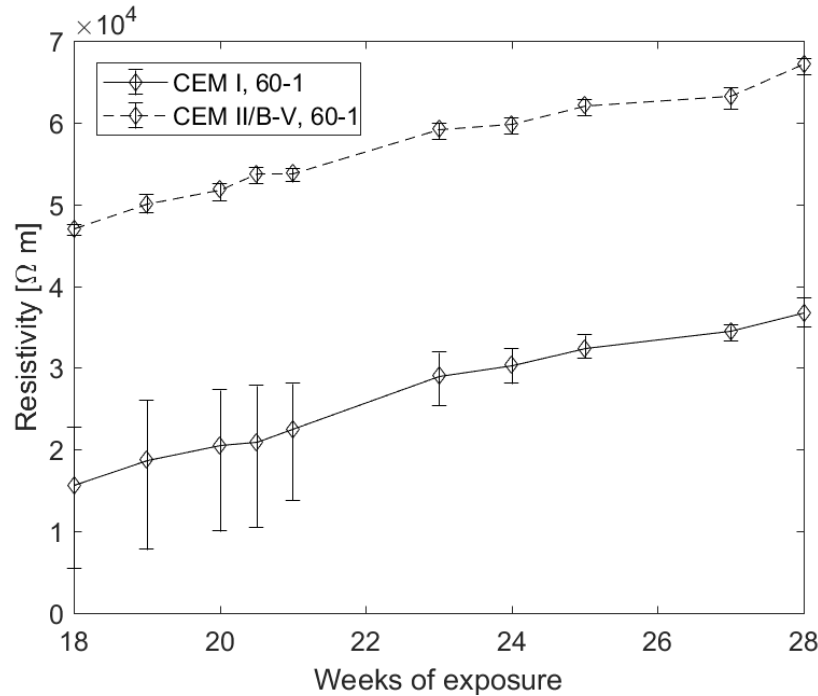
Figure 24: Resistivity of samples in different exposure conditions. The samples were cured for 2 weeks before exposure. Each line is average value of 3 samples.

4.3   Pore structure investigation

The PF-test was performed after 27 weeks of exposure on samples from all exposure conditions. The procedure is presented in Chapter 3 - Method, as well as the formulas used to calculate the different pore structure parameters. Figure 25a shows the water content in the samples after 27 weeks of exposure in percentage of sample weight. Figure 25b show the degree of capillary saturation in the samples. This is the actual water content in the samples, divided by the total pore volume. Figure 25c show the capillary pore volume in the samples. It is important to note that the pore volume estimated through this test is not the total pore volume (gel-pores, capillary pores and air voids), as the samples are only submerged in water and not pressure saturated. This means that the air voids are not filled in this test.

Each bar in figure 25 represents the average value of three samples. The sample weight was taken with an accuracy of 0.001 g. The average value is used in Figure 25, and the positive and negative error for each sample is shown in Table 20 in Appendix A.5. The full set of measurements is shown in Appendix A.8.

In Figure 25a the moisture content in weight percentage of the exposed samples are shown. The sealed samples show the highest moisture content at around 8 to 10 %. The samples from 90-0

shows a moisture content of about 8 %, 90-5 from 5 to 7 %, 60-0 from 5 to 6 % and 60-1 around 2 %.

Figure 25b show the degree of capillary saturation (DCS). The samples from 60-1 shows the lowest DCS at around 25 to 40 %. The samples from 60-0 show a DCS at around 50 %. In 90-5, CEM II/B-V has a DCS of 60 %, whereas CEM I has a DCS of 80 %. In 90-0, both cements has a value of 80-90 %, and the sealed samples has a DCS between 85 and 95 %.

Figure 25c show the porosity of the samples (the porosity accessed by water suction). The difference between CEM II/B-V and CEM I is similar in all conditions except for 90-5. The samples from 60-1 show the lowest porosity, followed by 90-5. 90-0, 60-0 and sealed conditions show somewhat similar results.
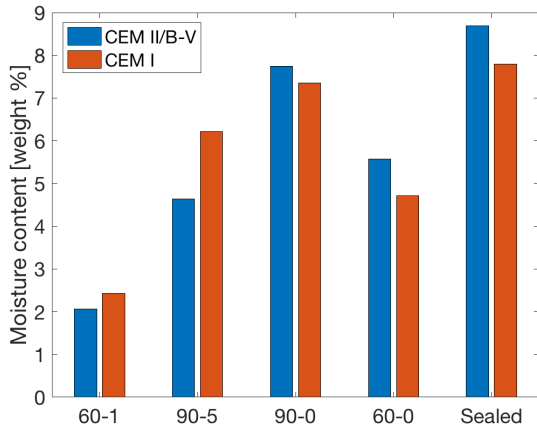
(a) Moisture content in samples after exposure to different RH and CO_2 conditions. Water content divided by sample weight.
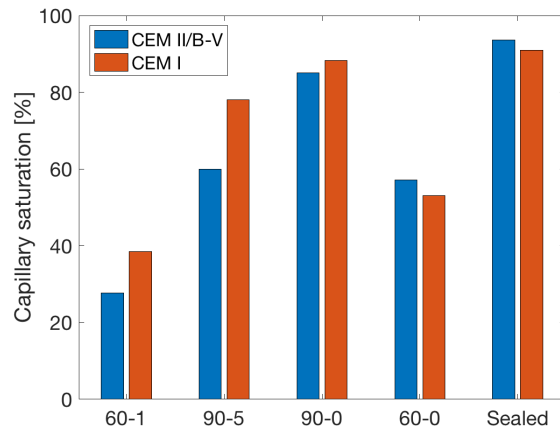
(b) Degree of capillary saturation. Moisture content divided by total pore volume.
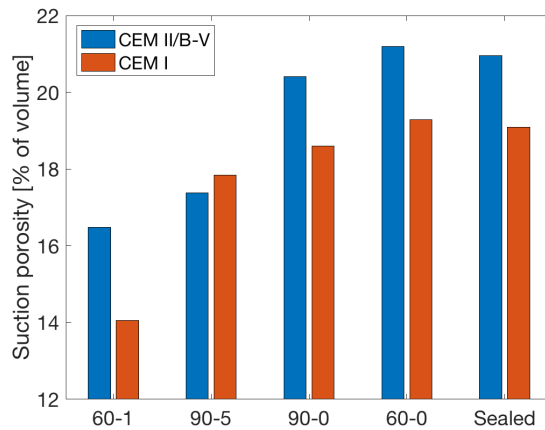
(c) Total pore volume. Water uptake divided by sample volume.

Figure 25: PF-testing of samples after 2 weeks of sealed curing and 27 weeks of exposure. Bars is average value of 3 samples. All calculations is done as described in Chapter 3.9

Figure 26 is a plot showing water content in samples (in weight %) plotted against different relative humidities. It shows the relationship between moisture content in the samples and the environment the samples are placed in.
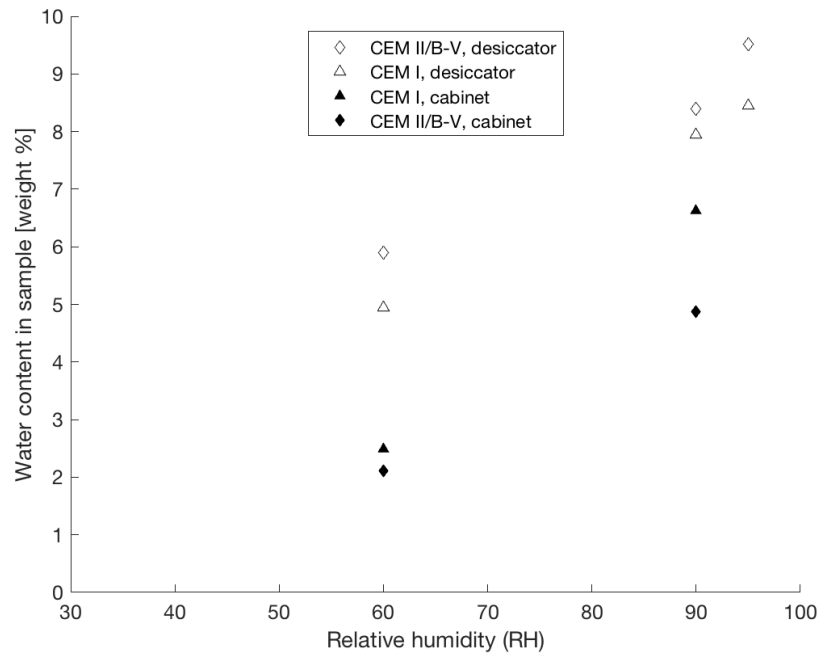
Figure 26: Water content in samples at different relative humidities and exposure conditions. Initial water content in weight %.

Table 15 show the difference between The first and last dry weight measured through the PF-test (W_2 - W_5). Each value is an average of 3 samples.

Table 15: The difference between W_2 and W_5 from PF-testing. All values in grams.

	60-1	90-5	90-0	60-0	Sealed
CEM I	0.035	-0.035	-0.030	-0.081	-0.009
CEM II/B-V	0.025	0.035	-0.029	-0.069	-0.037

4.4   Corrosion potential

Figure 27 and 28 show potential measurements taken once a week during exposure. The measurements were stopped after 28 weeks of exposure, since the other tests were performed after 27 weeks of exposure. The procedure for measuring are described in Chapter 3 - Method. The measurements are taken with an accuracy of 1 mV. Each line in Figure 27 and 28 are the average value of three samples. The error bars for each line represent the highest and lowest potential in the three samples. The full set of measurements are shown in Appendix A.3.
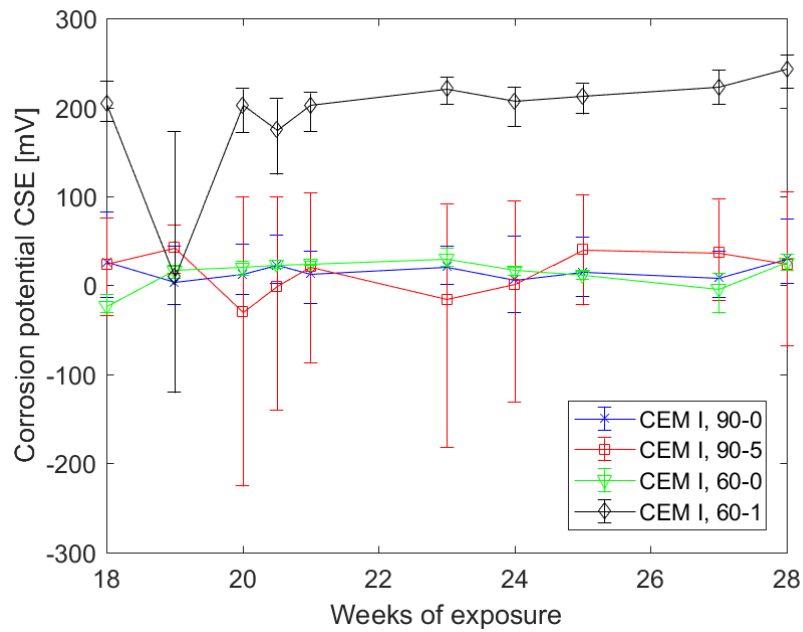
Figure 27: Corrosion potential of samples made with CEM I. Exposed after 2 weeks of sealed curing.
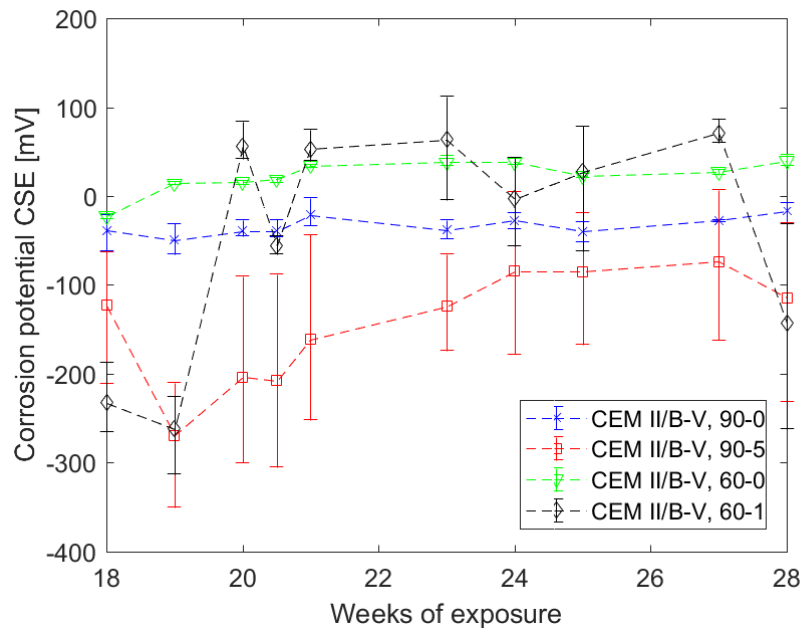
Figure 28: Corrosion potential of samples made with CEM II/B-V. Exposed after 2 weeks of sealed curing.

4.5   Pore solution investigation

After performing CWE and PSE as described in Chapter 3, the pore solution was sent to the Department of Chemistry, NTNU, for ICP-MS analysis. Syverin Lierhagen was responsible for performing the analysis. The raw data received from Syverin is shown in Appendix A.9.

ICP-MS was performed two times (two batches), 22.11.2017 and 14.12.2017. The first batch contained pore solution obtained through CWE from 60-1, 60-0, 90-0 and sealed conditions. The second batch contained pore solution obtained through CWE from 90-5 and pore solution obtained through PSE from sealed samples.

In the following figures, Equation 2 has been used to obtain the values. One simplification has been used, as the ratio between water and powder has been set equal to 1.

Figure 29 show the sodium and potassium concentration in the samples from 60-1, 90-0, 60-0 and sealed conditions. The samples from 60-1 show considerably lower concentrations than the other samples. For all the conditions, except 60-1, CEM II/B-V show a lower concentration of sodium and potassium than CEM I. This trend is stronger in 60-0 and 90-0 than in sealed condition, where CEM I and CEM II/B-V is more comparable.

Figure 30 show concentration of magnesium, iron, calcium, aluminum, sulfur and chlorine in the pore solution of samples from 60-1, 90-0, 60-0 and sealed conditions. The samples from 60-1 show considerably higher concentrations of sulfur and chlorine in Figure 30e and 30f than the other conditions.
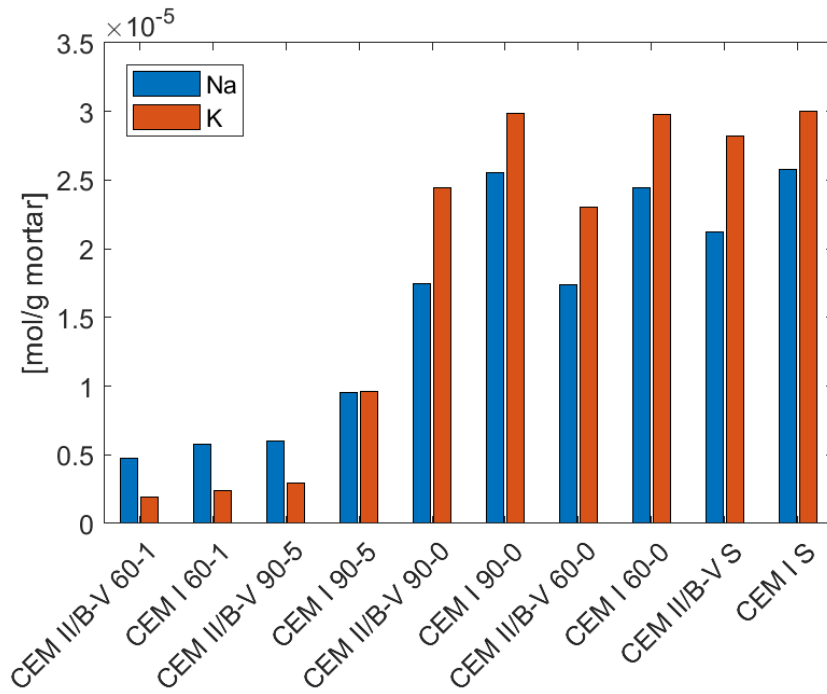
Figure 29: Sodium and Potassium concentrations obtained from CWE and ICP-MS after 2 weeks of sealed curing and 27 weeks of exposure.
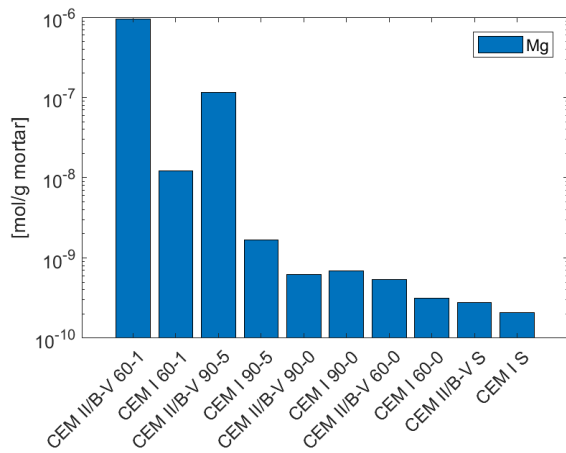
(a) Magnesium
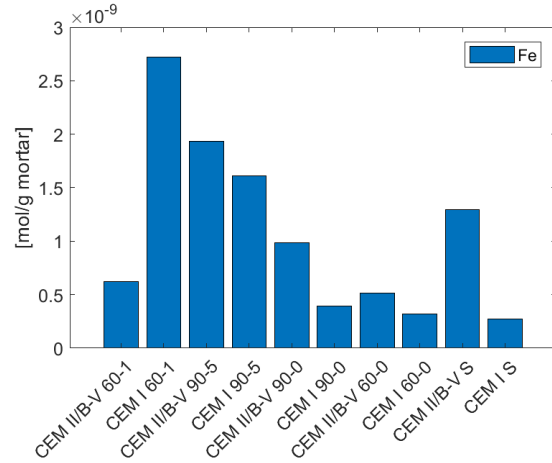
(b) Iron
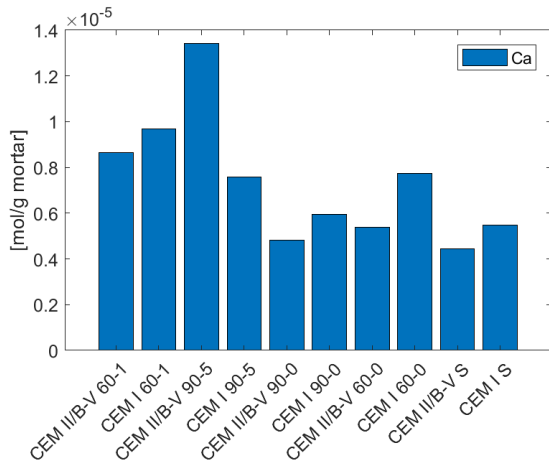
(c) Calcium
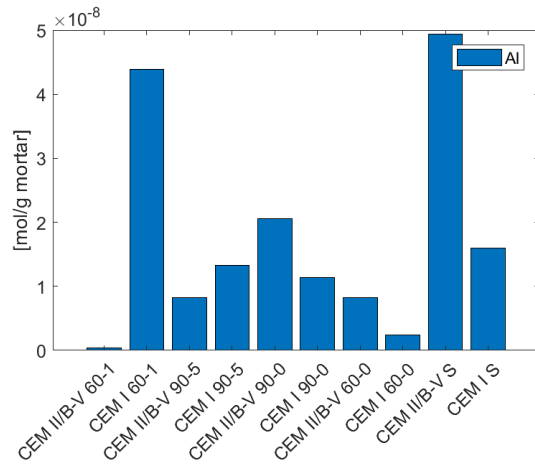
(d) Aluminum
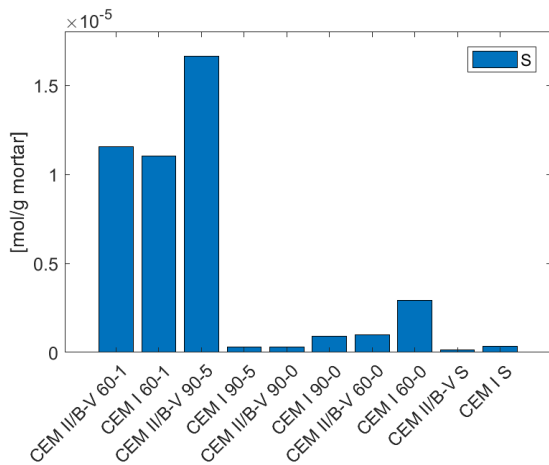
(e) Sulfur
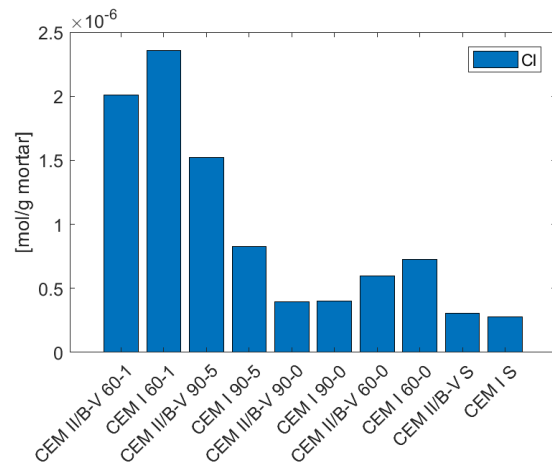
(f) Chlorine

Figure 30: Concentrations of different elements obtained from CWE and ICP-MS after 2 weeks of sealed curing and 27 weeks of exposure.

4.6   PSE vs. CWE

ICP-MS were performed on pore solution obtained from both PSE and CWE from sealed samples. CWE and PSE was performed after 29 weeks of sealed curing.

In the following figures Equation 3 and 4 has been used to calculate the values. For simplification, $m_{water\,added}$ and m_{powder} was both set to 20 g in Equation 3

Figure 31 and 32 show a comparison of the two methods CWE and PSE.
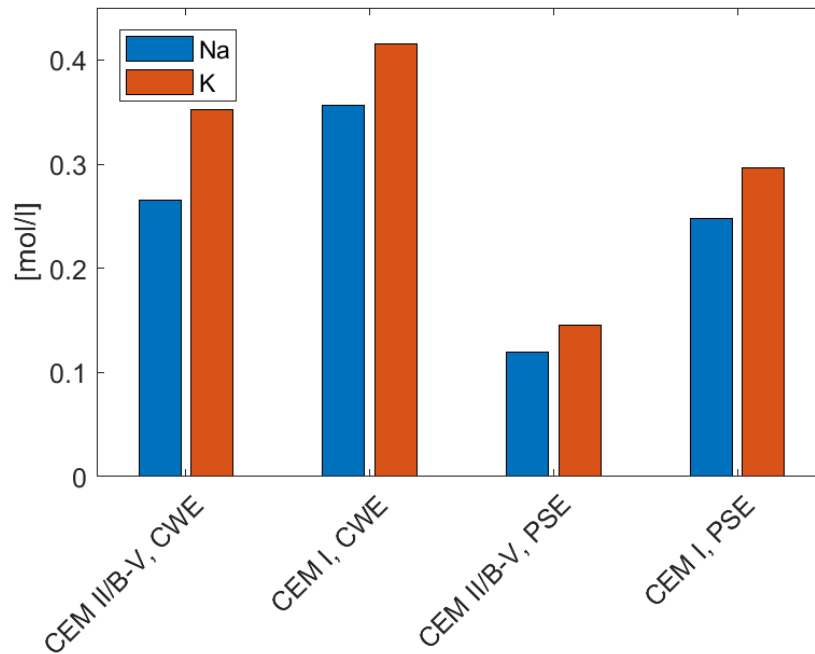
Figure 31: Sodium and Potassium concentrations obtained from ICP-MS. Pore solution obtained from CWE and PSE performed on sealed samples.

(a) Magnesium

(b) Iron

(c) Calcium

(d) Aluminum

(e) Sulfur

(f) Chlorine
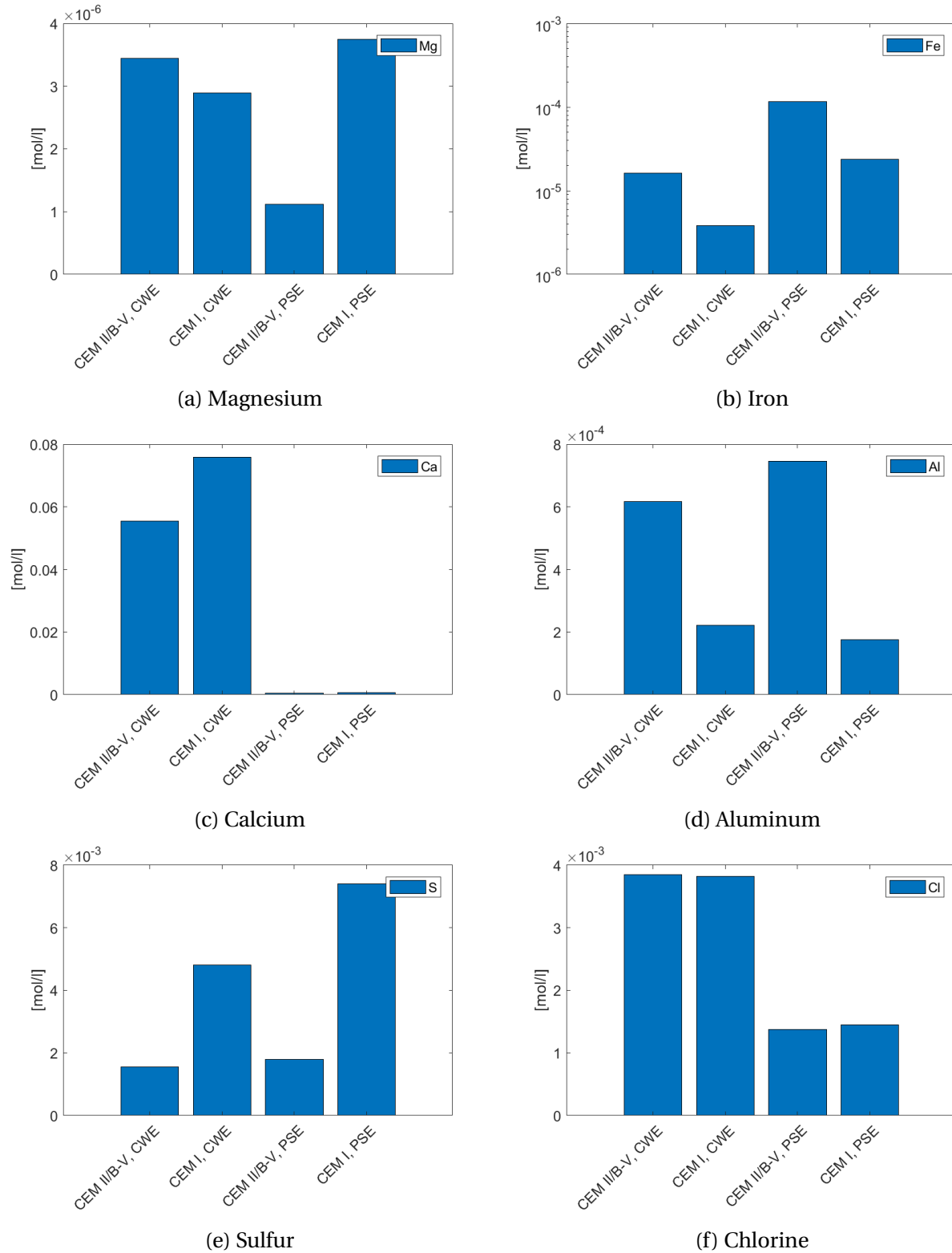
Figure 32: Concentrations of different elements obtained from ICP-MS after 29 weeks of sealed curing. Pore solution obtained by performing CWE and PSE on sealed samples.

5   Discussion

This thesis has investigated the resistivity, corrosion potential, pore structure and the pore solution composition of carbonated and non-carbonated mortar. As presented in Chapter 4, the effect of carbonation is clearly visible through extensive testing.

There has been some challenges throughout this thesis. It was early found that the samples dedicated for PSE were too dry to yield any pore solution, and therefore CWE was used as an alternative. PSE was still performed on sealed samples (that was found to hold enough moisture) and compared to CWE in order to compare the two methods and justify the usage of CWE.

The rate of carbonation was another obstacle that had to be dealt with. The initial plan was to have carbonated samples from two different moisture conditions, but the carbonation process in 90 % relative humidity was slower than anticipated, and the plan had to be changed. Some of the samples from 90-5 were crushed with a jaw-crusher and left in the carbonation cabinet for 8 weeks in the hope of speeding up the carbonation process. This was partly successful, as the fly ash samples showed nearly full carbonation, while the regular Portland cement samples showed only partial carbonation.

In this chapter the results are discussed. First, results from each test is discussed alone and compared to findings from other authors. Then, the results of the different tests are discussed together, and the relationship between them is shown.

5.1   Extent of carbonation

TGA was performed to determine the degree of carbonation in the samples and is shown in Figure 21 and 22. It was also performed to investigate the carbonation in the samples from 90-5 after they had been crushed and further carbonated for 8 weeks. The samples from 60-1 were used as reference in this test, as these samples appeared to be fully carbonated when spraying them with thymolphthalein. As suspected, the samples fro 60-1 showed no amount of CH, indicating full carbonation. Full carbonation was not achieved in the crushed CEM I 90-5, as seen in Figure 22, where there was found some CH in the samples. The crushed CEM II/B-V 90-5 however, show no CH and seems to be fully carbonated.

This means that all the samples from 60-1 used in all tests are fully carbonated, whereas the samples from 90-5 used in resistivity and corrosion potential measurements and the pore structure investigation were not investigated through TGA, and it is reasonable to assume that these samples are not fully carbonated at the time of testing.

5.2 Resistivity

Resistivity measurements were taken from 18 - 28 weeks of exposure, and showed a wide spread among the different samples. Figure 33 show resistivity values for all the samples. From this graph it is clear that moisture conditions, cement type and carbonation influences the resistivity.
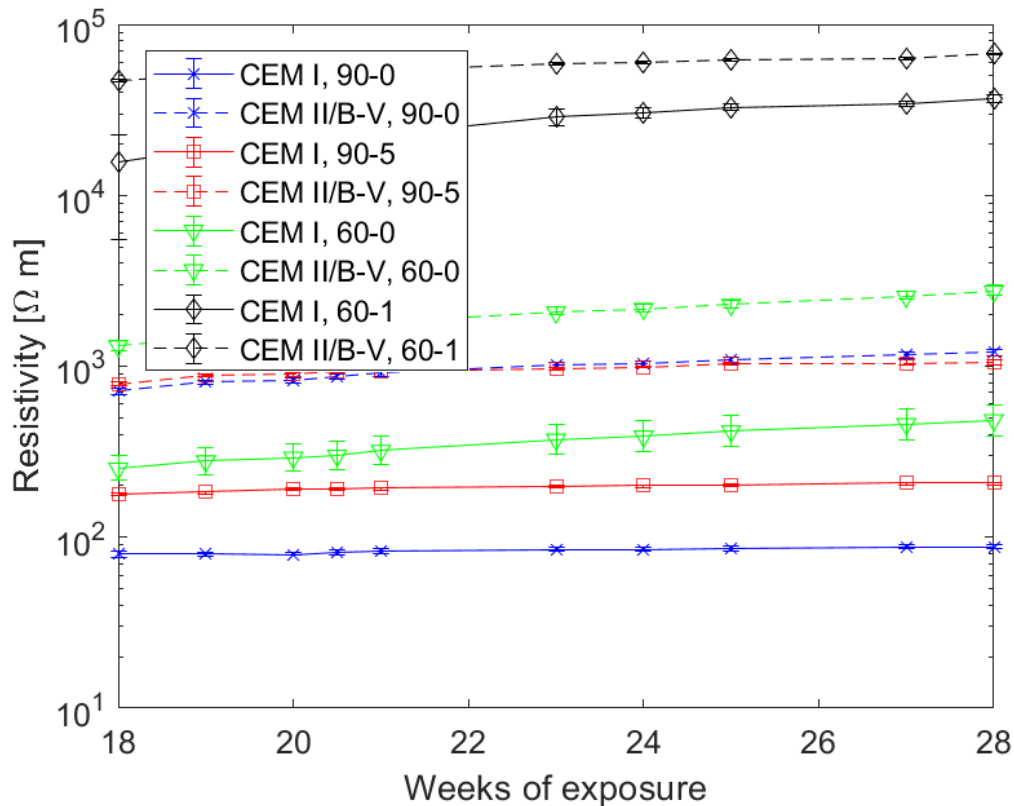
Figure 33: Resistivity in samples shown as a log-plot. Samples were cured sealed for 2 weeks before exposure. Each line is the average value of 3 samples, and the error bars show the highest and lowest value from the 3 samples.

Starting on the bottom of Figure 33, we clearly see that the CEM I samples from 90-0 and 90-5 is showing stable and low resistivity, indicating small or no change in the sample in the period of testing. Given that the CEM I 90-5 sample is showing almost the same resistivity as the sample from 90-0, this indicates that the sample has not yet carbonated. CEM I 60-0 shows a higher resistivity than CEM I 90-0, which makes sense, given that it is exposed to a lower relative humidity. The fact that it is steadily increasing could suggest that the samples is still drying. Since the sample started out with a moisture content much higher than 60 %, it will take a lot of time until the sample has stabilized at 60 %. This drying could still be happening, and be the reason for the increase in CEM I 60-0 compared to the stable lines of CEM I 90-0.

Moving over to the CEM II/B-V samples, some of the trends found in CEM I are also visible here, as the samples from 90-0 and 90-5 is stacked together, whereas CEM II/B-V 60-0 is increasing and visibly higher than 90-0 and 90-5. CEM II/B-V 90-5 is similar to 90-0, indicating, again, that the samples from 90-5 is not fully carbonated.

It is also worth noting that the resistivity is higher in CEM II/B-V compared to CEM I in all exposure conditions. This is in agreement with Medeiros-Junior et al. (2016) [29]. They state that the higher resistivity shown in fly ash blended cements is due to the less permeable pore structure and the pozzolanic reaction that is also lowering the permeability. From the findings in this thesis, the porosity of the fly ash blended samples is larger than than samples made with CEM I, suggesting that it is the interconnectivity of the pore structure rather than the pore volume that is determining the resistivity. That being said, the pore structure analysis in this thesis was performed six months after casting, and this might lead to a limited pozzolanic reaction, as Medeiros-Junior et al. show an increase in resistivity due to the pozzolanic reaction starting one year after casting.

The samples with the highest resistivity are the samples from 60-1, which also is the only fully carbonated samples (this is shown by TGA in Figure 21 and 22). This shows that carbonation increases the resistivity. Comparing the carbonated and non-carbonated samples in 60 % RH, there is an increase in resistivity by a factor of 25 in CEM II/B-V and by a factor of 80 in CEM I upon carbonation.

Comparing the resistivity values obtained in this thesis to Polder et al. (2001) [27] shown in Table 1. Polder et al. states that non-carbonated OPC *concrete* (20^oC/80%RH), shows a resistivity in the range of 200 - 500 Ω m. The findings in this thesis show a resistivity of 87±2.6 Ω m in OPC *mortar* (20^oC/90%RH) after 2 weeks of sealed curing and 27 weeks in 90-0. This is lower than the reference values given by Polder, but considering it is mortar and not concrete, it is expected to have a lower resistivity. For carbonated OPC concrete (20^oC/50%RH), Polder show a resistivity of 1000 Ω m and higher, whereas this thesis shows a resistivity of 36 763±1750 Ω m for OPC mortar after 2 weeks curing and 27 weeks in 60-1. This is much higher than the values given by Polder, especially considering Polder reports values for concrete, that should show a higher resistivity than mortars.

For non-carbonated fly ash (<25%) concrete, Polder reports resistivity in the range of 1000 - 4000 Ω m. This thesis reports resistivity of 1200±49 Ω m for CEM II/B-V in 90-0, which is in agreement. For carbonated fly ash concrete (20^oC/50%RH), Polder reports resistivity of 4000 - 10 000 Ω m, whereas the findings in this thesis is 67 190±1010 Ω m. This is again much higher than anticipated.

In summary, carbonation has shown to increase the resistivity of both CEM I and CEM II/B-V

significantly. In general, CEM I show a lower resistivity than CEM II/B-V in in each exposure condition. The samples from 60-0 is steadily increasing, most likely due to continuous drying at the time of testing. Carbonation seems to have a greater impact on the change of resistivity than the different cement types.

5.3   Pore structure investigation

In order to get an overview of the moisture content, degree of saturation and the pore volume in the samples, a simplified PF-test was performed on the samples after 27 weeks of exposure. Figure 25 show moisture content, degree of capillary saturation and total pore volume in the samples. All the characteristics were obtained as described in chapter 3.

When looking at the moisture content graph, Figure 25a, there is no surprise that the samples from 60 % RH are the ones with the lowest moisture content. The samples from 60-1 show the lowest moisture content, followed by 60-0, 90-5, 90-0 and sealed conditions. It seems that when exposed to CO_2, CEM II/B-V shows a lower moisture content compared to CEM I, whereas in the desiccators and sealed conditions CEM I show the lowest moisture content. The higher moisture content in CEM II/B-V in the non-carbonated samples could be explained by the lower amount of cement in CEM II/B-V compared to mortar made with CEM I. In other words, it seems that mortars made with CEM II/B-V become dryer than mortars made with CEM I when exposed to CO_2.

The pore volume of all the samples are shown in Figure 25c. Here it becomes clear that CO_2 exposure affects the pore volume. The samples from 60-1, which are carbonated, show a significant lower pore volume than samples from the other conditions. The samples from 90-0, 60-0 and sealed conditions show comparable pore volumes at around 19 % for CEM I and 21 % for CEM II/B-V. CEM II/B-V show a larger pore volume compared to CEM I in all conditions, which makes sense given the lower amount of cement in the fly ash samples compared to the CEM I samples. With less cement in the fly ash samples, there will be more excess water in these samples. This is visible in Figure 25a, where CEM II/B-V samples from desiccators and sealed conditions have a higher moisture content than samples made with CEM I.

The samples from non-carbonated environments all have comparable pore volumes for each binder, while the carbonated samples, from 60-1, have a distinctive lower pore volume. This is in agreement with Morandeau et al. (2014) [20], where cement pastes (both OPC and fly ash blended cements) showed a lower pore volume upon carbonation. It is also in agreement with Østnor et al. [30] which showed a decrease in pore volume upon carbonation. Østnor et al. found that for samples cured for 14 days (as is the case in this thesis) the pore volume in OPC samples decreased with 10 % upon carbonation, whereas fly ash samples decreased with 4 %

upon carbonation. The findings in this thesis show a decrease of 5 % for both CEM I and CEM II/B-V upon carbonation. It should however be noted that Østnor et al. used another method to determine the pore volume (MIP), so it is difficult to compare these results with the results obtained by the PF-method used in this thesis.

The samples from 90-5 show a pore volume in between the samples from 60-1 and 90-0, i.e. between the non-carbonated and the carbonated samples. The CEM II/B-V 90-5 has decreased in pore volume almost to the level of CEM II/B-V 60-1, which could indicate that this samples is partly carbonated, but that the core of the samples are still not carbonated given there is no change in resistivity. The CEM I 90-5 has not decreased in pore volume, and this could indicate that the process of carbonation goes slower in CEM I compared to CEM II/B-V, which was confirmed by TGA. This is in agreement with both the test-casting performed in my project thesis, and observations from TGA testing.

Figure 26 show the relationship between the relative humidity condition and the moisture content in the samples placed in said condition. It further substantiate that the samples made with CEM II/B-V seems to become dryer than samples made with CEM I when exposed to CO_2.

The last step in the PF-test is to dry the material at 105^oC and compare the weight against the first dry weighting. This is shown in Table 15. As shown, the weight change is relatively small, indicating that the material has not been destroyed during the testing.

The conclusion is that CO_2-exposure affects both the pore volume and moisture content. The mortars made with CEM II/B-V became dryer than mortars made with CEM I when exposed to CO_2, whereas the lowest moisture content in the non-carbonated samples were found in mortars made with CEM I. CEM II/B-V show a larger pore volume than than CEM I both before and after carbonation. The moisture content and pore volume of both cement types is reduced upon carbonation, but the difference in pore volume between mortars made with CEM II/B-V and CEM I stays relatively constant before and after carbonation.

5.4   Pore solution investigation

ICP-MS was performed on acidified filtrate obtained through CWE and on pore solution obtained through PSE as described in Chapter 3. A number of elements were analyzed, some of which are shown in this thesis. The full analysis is shown in Appendix A.9.

When analyzing the results obtained through ICP-MS, it is important to note the degree of carbonation in the different samples. All the samples from 60-1 are fully carbonated, this was confirmed through TGA. The samples from 90-5 were crushed into pieces the last 8 weeks of exposure in an attempt to achieve full carbonation, but this was not successful as they were

compared to 60-1 samples through TGA. The ICP-MS results for samples from 90-5 is therefore not comparable to the other samples, as they are not carbonated to the same extent.

Looking at the results in Figure 29 and 30, it is clear that carbonation causes a change in the pore solution composition. Especially for the alkali metals sodium and potassium this effect is substantial. Carbonated mortar of both cements show a alkali metal concentration of 1/3 to 1/4 of the non-carbonated alkali concentration. This is in agreement with the findings of Qi Pu et al. [28]. There seems to be more widespread results for other elements. The concentration of Na and K in 60-1 is similar for both cement types, indicating that the pore solution composition alone cannot explain the difference in resistivity in the different cements upon carbonation.

Comparing the results in this thesis to the results from De Weerdt et al. (2011) [10], some similarities can be found. Table 16 show a comparison of the pore solution composition from [10] and this thesis. De Weerdt et al. states that the concentrations of Na and K is lower in fly ash blended cements compared to pure Portland cements. This is also found in this thesis, shown in Figure 31 in the pore solution obtained through PSE. They also states that replacing OPC with fly ash reduces the sulphate concentration. The results from this thesis show that the concentration of sulfur is lower in CEM I compared to CEM II/B-V in non-carbonated samples, shown in Figure 32e in pore solution obtained through PSE. In carbonated samples however, sulfur seems to be released in the pore solution of both CEM I and CEM II/B-V, as shown in Figure 30e. The same is the case for chlorine in Figure 30f, which in a durability perspective is not ideal.

Table 16: Comparison of pore solution composition between this thesis and the findings of De Weerdt et al. (2011) [10]. For De weerdt et al.: OPC = 100 % Portland cement, OPC-FA = 65 % Portland cement and 35 % fly ash, cement paste samples (w/b = 0.5), both cements cured for 140 days and pore solution obtained through the steel die method (a form of PSE). For Langedal: mortar samples of CEM I and CEM II/B-V cured sealed for 203 days, pore solution obtained through PSE. Pore solution composition obtained by ICP-MS by both authors.

Author	Cement type	Concentration in pore solution [mmol/l]					
		Na	K	Ca	S	Si	Al
De Weerdt	OPC	302	565	1	13	0.3	0.33
Langedal	CEM I	247.5	296.0	0.7	7.4	4.97E-04	0.2
De Weerdt	OPC-FA	151	227	0.7	2.6	0.53	0.27
Langedal	CEM II/B-V	119.4	144.9	0.5	1.8	3.54E-04	0.7

To conclude, carbonation lowers the concentration of Na and K in the pore solution. This could be one of the reasons for the increase in resistivity upon carbonation. CEM I shows a higher content of Na and K in all non-carbonated samples, which could explain why CEM I show a lower

resistivity than CEM II/B-V in these conditions. Upon carbonation however, the concentration of Na and K is similar in CEM I and CEM II/B-V. Sulfur and chlorine seems to be released in the pore solution upon carbonation.

5.4.1 PSE vs. CWE

As described earlier in this thesis, many of the samples were too dry to yield any pore solution, and therefore CWE was introduced as a replacement to PSE. In order to justify the change of method, PSE and CWE were performed on sealed samples, which had enough moisture to yield pore solution.

As seen in Figure 31 and 32, pore solution obtained through CWE show higher concentration of sodium, potassium, calcium and chlorine compared to PSE. It would be interesting to see if this is the case in the other conditions as well, as chlorine seems to be released in the pore solution upon carbonation (according to CWE). The increase in PSE compared to CWE might be due to the dissolution of phases and that the CWE analysis is very sensitive to the determination of moisture content. When grinding and mixing samples through CWE, part of the sample will dissolve in the water. The amount of dissolved elements in the filtrate or the pore solution obtained through PSE will not necessarily represent the pore solution of an untouched sample.

Table 17 show the results of PSE and CWE for this thesis compared to the results of Plusquellec et al. (2017) [25]. Plusquellec et al. compared the pore solution composition obtained through different methods, PSE and CWE among others, using the same material used in this thesis (mortars of CEM I and CEM II/B-V with w/b = 0.5) cured in sealed conditions for 28 days. In this thesis the mortar-samples have been cured for 29 weeks.

Table 17: Comparison of results obtained by Plusquellec et al. [25] and the findings in this thesis (Langedal). Results obtained by ICP-MS analysis done on pore solution obtained by different methods. Curing time for the mortars was 28 days for Plusquellec et al. and 29 weeks for Langedal.

Id.	Method	Pore solution composition (mmol/l)											
		Na		K		Ca		Al		Si		S	
		Plusquellec	Langedal	Plusquellec	Langedal	Plusquellec	Langedal	Plusquellec	Langedal	Plusquellec	Langedal	Plusquellec	Langedal
CEM I	PSE	264	247	381	296	1.4	0.7	0.21	0.18	0.47	0.50	11.1	7.4
	CWE	320	356	400	416	100	76	0.14	0.22	0.28	N.A	3.8	4.8
CEM II/B-V	PSE	143	119	209	145	1.5	0.5	0.5	0.75	0.6	0.35	4.3	1.8
	CWE	188	265	240	352	70	56	0.25	0.62	0.4	N.A	1.6	1.6

As shown in Table 17, the findings in this thesis is comparable to the findings of Plusquellec et al. [25] even though the curing time is not the same for the two cases. For CEM II/B-V the concentration of Na and K are lower in this thesis than the findings of Plusquellec et al. This

difference could be due to the pozzolanic reaction of fly ash, as Plusquellec's samples were only cured for 28 days.

CWE obtained pore solution show a much higher concentration of calcium compared to pore solution obtained through PSE. This is the case both in this thesis and in the findings from Plusquellec et al. [25]. When mixing the grinded sample and water in the CWE procedure, calcium from the sample itself in the form of portlandite, causing a higher calcium concentration than the *real* pore solution concentration. When performing PSE, only the calcium dissolved in the pore solution itself is obtained, resulting in a lower (and truer) concentration.

5.5   Relation between resistivity, porosity, moisture content and pore solution composition

From the results in this thesis, it seems that carbonation, moisture content, cement type and pore solution composition influences the resistivity. In general, the CEM I samples shows a lower resistivity than the CEM II/B-V samples, even though the pore volume is lower in the mortars made with CEM I. The pore size distribution is not obtained through the tests performed, so no conclusion regarding the interconnectivity in the pore structure can be made. The pore solution of non-carbonated samples made with CEM I also show a higher concentration of Na and K compared to non-carbonated CEM II/B-V, which could explain the difference in resistivity. Also, CEM II/B-V samples show a lower degree of capillary saturation than CEM I samples, meaning a less water-filled pore structure, increasing the resistance.

When looking at the results from the pore structure investigation and the pore solution investigation on carbonated samples from 60-1, it becomes clear why they show such a large resistivity compared to the non-carbonated samples. The carbonated samples show a decrease in pore volume, degree of capillary saturation and the in the concentration of Na and K. This means a denser material with less water in it, making it "hard" for the ions in the pore water to carry the current around in the sample. The decrease of the alkali metals Na and K means less ions in the already reduced amount of pore water, which results in a higher resistivity.

The ratio in resistivity of mortars made with CEM I and CEM II/B-V is smaller in carbonated mortar (a factor of 1.8) than in non-carbonated mortar (a factor of 5.6), meaning that carbonation has a much bigger impact on resistivity compared to the cement types themselves. The Na and K concentration is also similar in the two cements after carbonation, whereas a difference can be seen in non-carbonated mortar.

In Figure 36 the resistivity is plotted against the alkali content in the samples. The samples from 90-5 is not included in this figure, as they are not comparable to the resistivity measurements,

because of the different pre-treatment of the samples in the two cases. From Figure 36 it is a clear relationship between resistivity and the concentration of alkalies in the samples, as a decrease in Na and K leads to an increase in resistivity.

In Figure 35 and 34 the resistivity is plotted against moisture content and degree of capillary saturation. The samples were sorted by resistivity, lowest to highest, and then plotted with the corresponding moisture and degree of saturation to show the relation between the characteristics. As seen in the figures, there is a good coherency between the samples made with CEM I. For CEM II/B-V, the relation is not as clear, as the sample from 905 deviates from the rest. One explanation could be that carbonation cause a pore structure- and moisture change in the samples, but since the change has not yet reached the core of the samples it is not visible in the resistivity. This is not an issue in the CEM I samples, as CEM I 90-5 has an even lower degree of carbonation (and corresponding small changes due to carbonation) than CEM II/B-V 90-5. Even so, there is a clear relationship between moisture content, capillary saturation and resistivity. As the moisture content decreases, the resistivity increases. The same is the case for the capillary saturation.
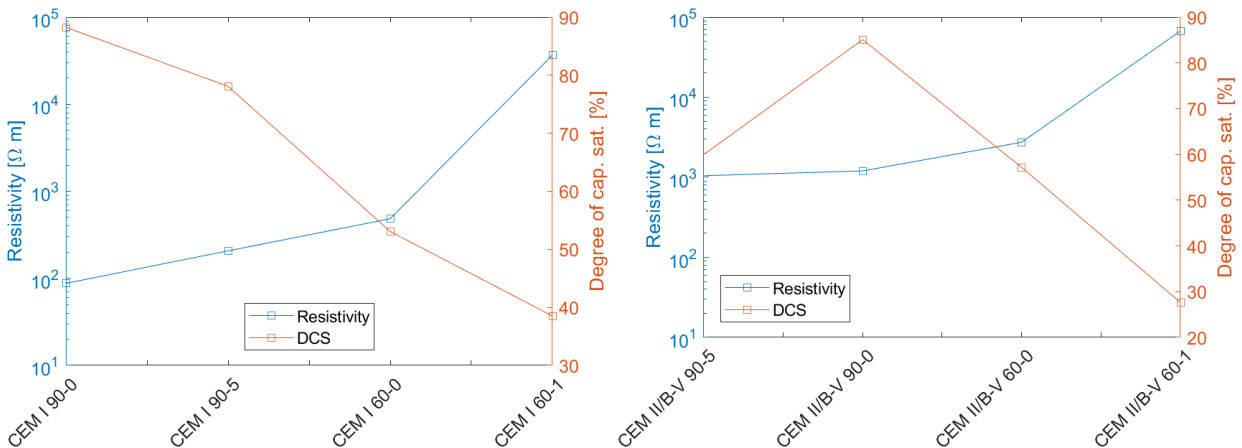
(a) Resistivity against degree of capillary saturation in CEM I samples.

(b) Resistivity against degree of capillary saturation in CEM II/B-V samples.

Figure 34: Resistivity against degree of capillary saturation.
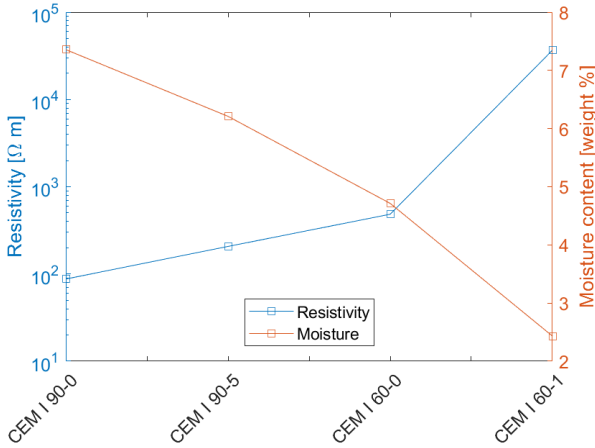
(a) Resistivity against moisture content in samples made with CEM I.
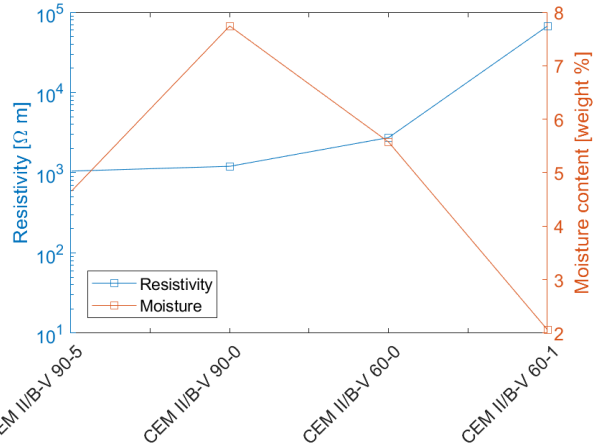
(b) Resistivity against moisture content in samples made with CEM II/B-V samples.

Figure 35: Resistivity against moisture content.
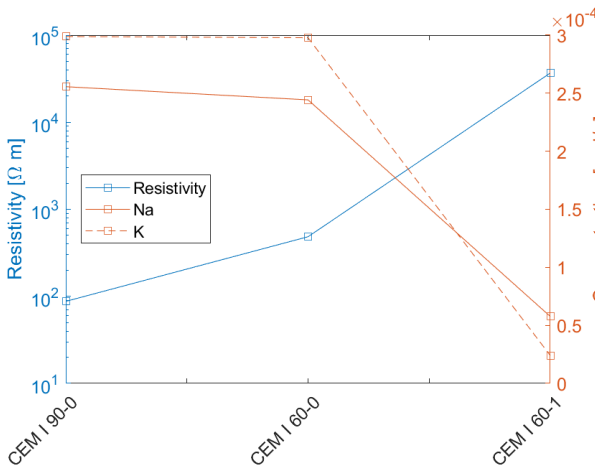
(a) Resistivity against alkali content in samples made with CEM I.
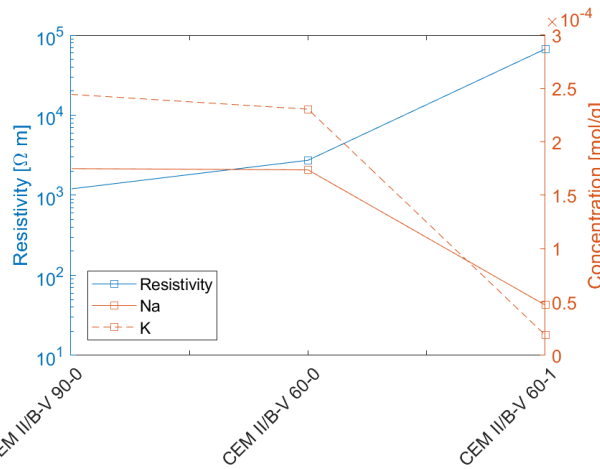
(b) Resistivity against alkalies in samples made with CEM II/B-V samples.

Figure 36: Resistivity against alkali concentration.

Overall, there seems to be a correlation between moisture content, degree of capillary saturation, pore solution composition and resistivity. It is though difficult to say which factor is the decisive one when it comes to resistivity, as both alkali content, moisture content and degree of capillary saturation is directly related to resistivity, where the lowest moisture content and alkali content correspond to the highest resistivity and vice versa.

With only carbonated samples from 60 % RH, it is difficult to say which parameter influences the resistivity the most, as is it only possible to compare results for samples in 60-1 and 60-

0. With carbonated samples from 90 % RH, it could be possible to determine how much each parameter affects the resistivity as this would give carbonated samples with a higher moisture content than the samples from 60-1. This could draw a better picture on how moisture content affects resistivity compared to the pore solution composition.

6   Conclusion

Mortars made with CEM I and CEM II/B-V was cured sealed for 2 weeks, then exposed to different relative humidity and CO_2-concentration for 27 weeks. The resistivity was measured using embedded titanium bars in the mortar samples. The pore structure was investigated using the PF-method. The extent of carbonation was measured using thermogravimetric analysis. The pore solution composition was investigated with cold water extraction and pore solution expression followed by analysis by ICP-MS.

Due to the low extent of carbonation in the samples stored in 90 % RH and 5 % CO_2, this thesis cannot at this point show the relationship between the resistivity of carbonated samples at different RH.

The resistivity of mortars made with CEM II/B-V were found to be higher than mortars made with CEM I, by a factor of 1.8 in carbonated state and by a factor of 5.6 in non-carbonated state. The resistivity was significantly higher in carbonated mortar than non-carbonated mortar for both cements. The ratio of resistivity between CEM I and CEM II/B-V was smaller in the carbonated state than the non-carbonated state, indicating that carbonation may have a greater impact on resistivity than the type of cement has.

Carbonation decreased the moisture content and pore volume in the mortars from both cement types. The mortars made with CEM II/B-V showed a larger pore volume than mortars made with CEM I in all exposure conditions. The degree of capillary saturation was related to the resistivity, as a lower degree of saturation corresponded to a higher resistivity.

The pore solution composition changed upon carbonation. A significant drop in the concentration of Na and K was seen upon carbonation. In the non-carbonated samples, the samples from CEM I showed a higher content of Na and K compared to samples from CEM II/B-V, whereas the Na and K content was similar for both cement types after carbonation.

Both moisture content, degree of capillary saturation and pore solution composition appears to influence the resistivity, but it is not possible to conclude to which extent each parameter influences the resistivity.

7 Further research

Overview of remaining samples and their placement is shown in Table 18.

After full carbonation is achieved in the cabinets, it would be interesting to look at the corrosion potential in the reinforced samples. If corrosion is happening, it could also be interesting to open the samples and compare the weight of the reinforcement with the initial weight provided in this thesis. Also, as the samples are carbonated, they could be placed in water and the corrosion rate and resistivity could be measured as the samples are drying. This could indicate how moisture-sensitive the corrosion- potential and rate is and how the resistivity is connected to corrosion.

After concluding this thesis, samples from 90-5 were again crushed and left in the cabinet to achieve full carbonation. These samples should be run through CWE and ICP-MS in order to have comparison of the pore solution composition from carbonated samples both at 60 % and 90 % RH.

From the ICP-MS raw data it is possible to calculate the pH and the pore solution resistivity. This could be done in order to compare bulk- and pore solution resistivity of the samples. This could help understand what the decisive factor is when it comes to resistivity; pore structure, pore volume, moisture, alkali concentration etc.

The pore structure investigation performed in this thesis is limited, due to the time available. I recommend to perform a full PF-method, with pressure saturation and maybe also drying at 50 ^oC in order to get a better picture of the porosity in the samples. MIP could also be interesting to look into, as the pore size distribution could tell a lot about how carbonation affect pores in different sizes.

References

[1] (10.06.2015). Wuxi advanced titanium technology co.,. *http://www.adv-ti.com.*

[2] Anstice, D.J., e. a. (2005). The pore solution phase of carbonated cement pastes. *Cement and Concrete Research*, 35(2):377–383.

[3] ASTM (2009). Standard test method for corrosion potentials of uncoated reinforcing steel in concrete. *C876 09.*

[4] Azarsa, P. and Gupta, R. (2017). Electrical resistivity of concrete for durability evaluation: A review. *Department of Civil Engineering, University of Victoria, Victoria, BC, Canada.*

[5] Behnood, A., e. a. (2016). Methods for measuring ph in concrete: A review. *Construction and Building Materials*, 105:176–188.

[6] Berodier, E., e. a. (2016a). *A Practical Guide to Microstructural Analysis of Cementitious Materials*, chapter 9 - Mercury intrusion porosimetry, pages 419–442. CRC Press.

[7] Berodier, E., e. a. (2016b). *A Practical Guide to Microstructural Analysis of Cementitious Materials*, chapter 5 - Thermogravimetric analysis, pages 177–208. CRC Press.

[8] Bertolini L., Elsener B., e. a. (2013). *Corrosion of Steel in Concrete - Prevention, Diagnosis, Repair.* WILEY-VCH.

[9] Cyr, M., e. a. (2008). High-pressure device for fluid extraction from porous materials: Application to cement-based materials. *Journal of the American Ceramic Society*, 91(8):2653–2658.

[10] De Weerdt, K., e. a. (2011a). Hydration mechanisms of ternary portland cements containing limestone powder and fly ash. *Cement and Concrete Research*, 41:279–291.

[11] De Weerdt, K., e. a. (2011b). Synergy between fly ash and limestone powder in ternary cements. *Cement & Concrete Composites*, 33:30–38.

[12] De Weerdt, K., G. M. and Orsakova, D. (2014). Investigation of concrete from solsvik field station. *NPRA reports.*

[13] Elkey, W. and Sellevold, E. J. (1995). Electrical resisivity of concrete. *Directorate of public roads, Norwegian Road Research Laboratory*, 80.

[14] Elsener, B., e. a. (2003). Half-cell potential measurements- potential mapping on reinforced concrete structures. *RILEM TC 154-EMC: 'Electrochemical Techniques for Measuring Metallic Corrosion'*, 36:461–471.

[15] Gjørv O.E., Vennesland Ø., E.-B. A. (1977). Electrical resistivity of concrete in the oceans. *Offshore Technology Conference*, 2803.

[16] Hornbostel, K. (2015). *The role of concrete resistivity in chloride-induced macro-cell corrosion.* PhD thesis, NTNU.

[17] Jacobsen, S., e. a. (2016). *TKT 4215 - Concrete Technology 1 - Kompendium.* NTNU - Institutt for konstruksjonsteknikk.

[18] MERCH (2017a). Barium chloride dihydrate for analysis emsure® acs, iso, reag. ph eur. SAFETY DATA SHEET - according to Regulation (EC) No. 1907/2006.

[19] MERCH (2017b). Sodium bromide 99.995 suprapur®. SAFETY DATA SHEET - according to Regulation (EC) No. 1907/2006.

[20] Morandeau, A., Thiéry, M., and et al. (2014). Investigation of the carbonation mechanism of ch and c-s-h in terms of kinetics, microstructure changes and moisture properties. *Cement and Concrete Research*, 56:153–170.

[21] Morandeau, A., Thiéry, M., and et al. (2015). Impact of accelerated carbonation on opc cement paste blended with fly ash. *Cement and Concrete Research*, 67:226–236.

[22] NORCEM (31.03.2015). Report on quality test.

[23] Normensand (13.05.2017). *http://normensand.de/en/products/cen-standard-sand-en-196-1/.*

[24] Pihlajavaara, S. E. (1968). Some results of the effect of carbonation on the porosity and pore size distribution of cement paste. *Matériaux et constructions*, 1(6):521–527.

[25] Plusquellec, G., e. a. (2017). Determination of the ph and the free alkali metal content in the pore solution of concrete: Review and experimental comparison. *Cement and Concrete Research*, 96:13–26.

[26] Plusquellec, G. and De Weerdt, K. (2017). Cold water extraction (cwe) - procedure for the determination of the alkali content and pore solution composition.

[27] Polder, R. B. (2001). Test methods for on site measurement of resistivity of concrete - a rilem tc-154 technical recommendation. *Construction and Building Materials*, 15:125–131.

[28] Qi Pu, Linhua Jiang, J. X. H. C. Y. X. Y. Z. (2012). Evolution of ph and chemical composition of pore solution in carbonated concrete. 28.

[29] Ronaldo A. Medeiros-Junior, M. G. L. (2016). Electrical resistivity of unsaturated concrete using different types of cement. *Construction and Building Materials*, 107:11–16.

[30] Tone Østnor, H. J. Lowcarbcem 2a – carbonation mechanism.

[31] Vollpracht, A., e. a. (2015). The pore solution of blended cements: a review. *Materials and Structures,* 49(8):3341–3367.

A   Appendix A

This Appendix contains raw data and additional information regarding testing and calculations done throughout the work of this thesis.

A.1   Remaining samples

Table 18: Remaining samples in cabinets and desiccators.

60-0			90-0		
3-1-1	-	-	-	-	1-2-3
-	-	3-2-3	-	-	1-3-3
-	-	3-3-3	-	-	1-4-3
-	-	3-4-3	-	1-5-2	1-5-3
3-5-1	3-5-2	3-5-3	5-1-1	5-1-2	5-1-3
7-1-1	7-1-2	7-1-3	-	-	5-2-3
-	-	7-2-3	-	-	5-3-3
-	-	7-3-3	5-5-1	5-5-2	5-5-3
7-5-1	7-5-2	7-5-3			

60-1			90-5		
-	-	4-1-3	-	-	2-1-3
-	-	4-2-3	-	-	2-2-3
-	-	4-3-3	-	-	2-3-3
-	-	4-4-3	-	2-5-2	2-5-3
4-5-1	4-5-2	4-5-3	-	-	6-1-3
-	8-1-2	8-1-3	-	-	6-2-3
-	-	8-2-3	-	-	6-3-3
-	-	8-3-3	-	6-5-2	6-5-3
-	-	8-4-3			
8-5-1	8-5-2	8-5-3			

A.2   Weight of reinforcement bars

Table 19: Reinforcement weights and placement. As for the labeling of samples, 1 is bottom and 3 is top.

Batch	Sample	Cement type	Reinforcement bar [g]		
			1	2	3
1	1	CEM II/B-V	28.257	28.924	29.513
2	2	CEM II/B-V	29.904	26.413	28.782
3	3	CEM II/B-V	27.517	30.016	28.613
4	4	CEM II/B-V	30.496	30.481	27.975
5	5	CEM I	28.873	28.206	27.365
6	6	CEM I	28.279	30.369	28.122
7	7	CEM I	27.502	29.324	28.384
8	8	CEM I	29.056	29.751	29.254

A.3   Potential measurements

Disc	Cement	RH	CO_2	12/09/2017		20/09/2017		26/09/2017		27/09/2017	
				Pot	Avg	Pot	Avg	Pot	Avg	Pot	Avg
1-7-1				-62		-65		-45		-46	
1-7-2	CEM II/B-V	90	0	-33.4	-38.8	-31	-49.666667	-27	-39	-26	-39.333333
1-7-3				-21		-53		-45		-46	
2-7-1				-211		-350		-300		-305	
2-7-2	CEM II/B-V	90	5	-95	-123	-248	-269.33333	-222	-204	-230	-207.66667
2-7-3				-63		-210		-90		-88	
3-7-1				-20		14		13		20	
3-7-2	CEM II/B-V	60	0	-23	-22.666667	12.6	14.2	17	16	15	18.6666667
3-7-3				-25		16		18		21	
4-6-1				-245		-247		42		-65	
4-6-2	CEM II/B-V	60	1	-265	-232.33333	-313	-261.66667	43	56.3333333	-57	-55.666667
4-6-3				-187		-225		84		-45	
5-6-1				82		44		46		56	
5-6-2	CEM I	90	0	-14	26	-22	3.66666667	-10	12.8333333	1.8	22.6
5-6-3				10		-11		2.5		10	
6-6-1				-34		46		-225		-140	
6-6-2	CEM I	90	5	30	24	14	42.6666667	36	-29.666667	37	-1
6-6-3				76		68		100		100	
7-6-1				-31		23		24		28	
7-6-2	CEM I	60	0	-28	-23	7.5	17.1666667	11	20.6666667	19	23.6666667
7-6-3				-10		21		27		24	
8-6-1				199		-120		172		125	
8-6-2	CEM I	60	1	230	204.333333	-23	10	215	202.666667	190	175
8-6-3				184		173		221		210	

Figure 37: Corrosion potential measurements. Part 1

04/10/2017		20/10/2017		26/10/2017		02/11/2017		13/11/2017	
Pot	Avg	Pot	Avg	Pot	Avg	Pot	Avg	Pot	Avg
-33		-48		-37		-51		-27	
-2	-21	-27	-38.333333	-19	-27.333333	-39	-39.666667	-26	-27.333333
-28		-40		-26		-29		-29	
-252		-174		-178		-167		-162	
-189	-161.33333	-133	-124	-80	-84.333333	-69	-85	-67	-74
-43		-65		5		-19		7	
36		34		42		21		30	
32	34.3333333	34	38	37	38.3333333	25	22.6666667	27	27
35		46		36		22		24	
44		-4		43		-62		60	
40	53	83	63.6666667	-56	-3.3333333	65	27.3333333	66	71
75		112		3		79		87	
38		44		55		54		38	
-20	13.3333333	1	21.3333333	-6	6.3333333	-12	15	-14	8.6666667
22		19		-30		3		2	
-87		-182		-131		-22		-17	
46	21	44	-15.666667	41	1.6666667	42	40.6666667	31	37
104		91		95		102		97	
27		28		20		16		-31	
23	24.6666667	21	30.3333333	11	17	7	12	6	-4
24		42		20		13		13	
173		204		179		193		204	
217	202.333333	234	221	219	207	219	213	222	222.666667
217		225		223		227		242	

Figure 38: Corrosion potential measurements. Part 2

22/11/2017		29/11/2017	
Pot	Avg	Pot	Avg
-30		-44	-29.333333
-7	-16.666667	-27	
-13		-17	
-231		-343	-135.33333
-82	-114.33333	-73	
-30		10	
47		51	33.3333333
38	39.6666667	31	
34		18	
-262		70	66
-135	-142.66667	57	
-31		71	
75		64	18.3333333
2	30.3333333	1	
14		-10	
-68		-10	49
35	24	44	
105		113	
27		37	39
17	26.3333333	36	
35		44	
222		218	242.666667
249	243.333333	244	
259		266	

Figure 39: Corrosion potential measurements. Part 3

A.4   Resistance measurements

				week	18		week	19		week	20	
				12.09.2017			20.09.2017			26.09.2017		
Disc	Cement type	RH [%]	CO₂	Frequenzy [kHz]	Angle [deg]	Resistance [kΩ]	Frequency [kHz]	Angle [deg]	Resistance [kΩ]	Frequenzy [kHz]	Angle [deg]	Resistance [kΩ]
1-6-1				1	-2	28.83	1	-2.1	32.78	1	-2.3	33.29
1-6-2	CEM II/B-V	90	0			29.76	1	-2.3	34.98	1	-2.5	35.85
1-6-3						31.42	1	-2.2	34.69	1	-2.3	35.25
2-6-1				10	-2	32.94	1	-3.1	37.57	1	-3.4	38.65
2-6-2	CEM II/B-V	90	5			34.3	1	-3.2	37.92	1	-3.3	38.35
2-6-3						32.17	1	-3.5	36.7	1	-3.6	36.87
3-6-1				1	-2.8	53.24	1	-2.9	59.02	0.12	-3	65.26
3-6-2	CEM II/B-V	60	0			59.85	1	-2.7	65.93	0.12	-2.8	73.31
3-6-3						52.07	1	-2.6	59.18	0.12	-2.7	65.6
4-7-1				100	-2.9	1990.8	0.1	0	2106	0.1	-0.1	2205
4-7-2	CEM II/B-V	60	1			1940	0.1	0	2056	0.1	-0.1	2120
4-7-3						1997.3	0.1	0	2152	0.1	-0.1	2209
5-7-1				1	-1.6	3.461	10	-0.9	3.443	10	-1.1	3.4
5-7-2	CEM I	90	0			3.337	10	-0.8	3.335	10	-1	3.3
5-7-3						3.221	10	-0.9	3.246	10	-1	3.3
6-7-1				10	-1.9	7.603	10	-2.2	7.786	1	-2.6	8.2
6-7-2	CEM I	90	5			7.496	10	-2	7.786	1	-2.5	8.16
6-7-3						7.324	10	-1.8	7.552	1	-2.2	7.86
7-7-1				1	-1.2	12.58	1	-1.2	14	1	-1.2	14.8
7-7-2	CEM I	60	0			10.17	1	-1.5	11.3	1	-1.6	11.76
7-7-3						9	1	-1	9.77	1	-1	10.26
8-7-1				100	-2.9	955.7	0.1	-3.1	1096	0.1	-3.5	1147
8-7-2	CEM I	60	1			782.7	0.1	-3.1	936	0.1	-3.5	1016
8-7-3						232	0.1	-2	328.5	0.1	-2.5	421

Figure 40: Resistance measurements. Part 1

week	20.5		week	21		week	23		week	24	
27.09.2017			04.10.2017			19.10.2017			26.10.2017		
Frequency [kHz]	Angle [deg]	Resistance [kΩ]	Frequenzy [kHz]	Angle [deg]	Resistance [kΩ]	Frequency [kHz]	Angle [deg]	Resistance [kΩ]	Frequenzy [kHz]	Angle [deg]	Resistance [kΩ]
1	-2.3	35.08	1	-2.3	36.79	1	-2.4	41.06	1	-2.3	41.86
1	-2.5	37.83	1	-2.5	39.51	1	-2.7	44.11	1	-2.5	45
1	-2.4	36.83	1	-2.3	38.57	1	-2.5	42.5	1	-2.4	44.11
1	-3.4	40.08	1	-3.4	40.09	1	-3.5	40.94	1	-3.4	41.8
1	-3.4	39.56	1	-3.3	39.42	1	-3.4	40.1	1	-3.3	41
1	-3.7	38.42	1	-3.7	38.93	1	-3.8	40.77	1	-3.7	41.9
0.12	-3	67.02	0.1	-3	72.23	0.1	-3	83.72	0.1	-3	87.55
0.12	-2.8	75.41	0.1	-2.8	81.07	0.1	-2.8	93.33	0.1	-2.8	97.5
0.12	-2.7	67.5	0.1	-2.8	72.98	0.1	-2.7	83.88	0.1	-2.7	88.1
0.1	0.1	2278	0.1	-0.1	2278	0.1	-0.1	2520	0.1	-0.1	2543
0.1	-0.1	2208	0.1	-0.1	2217	0.1	-0.1	2437	0.1	-0.1	2463
0.1	-0.1	2291	0.1	-0.1	2286	0.1	-0.1	2505	0.1	-0.1	2535
1	-2.5	3.54	1	-1.6	3.6	1	-1.6	3.69	1	-1.6	3.68
1	-1.4	3.46	1	-1.3	3.47	1	-1.3	3.555	1	-1.4	3.529
1	-2.8	3.31	1	-1.4	3.38	1	-1.4	3.464	1	-1.4	3.455
1	-2.7	8.21	1	-2.6	8.24	1	-2.7	8.472	1	-2.6	8.525
1	-2.6	8.19	1	-2.5	8.24	1	-2.5	8.471	1	-2.5	8.522
1	-2.2	7.9	1	-2.2	7.93	1	-2.2	8.177	1	-2.2	8.16
1	-1.3	15.26	1	-1.2	16.38	1	-1.3	19.15	1	-1.3	20.1
1	-1.6	12.03	1	-1.5	12.85	1	-1.6	14.9	1	-1.6	15.6
1	-1.1	10.5	1	-1	11.11	1	-1.1	12.89	1	-1	13.33
0.1	-3.7	1169	0.1	-3.6	1181	0.1	-4	1343	0.1	-4.1	1362
0.1	-3.7	1031	0.1	-3.7	1077	0.1	-4.1	1248	0.1	-4.2	1282
0.1	-2.6	441	0.1	-3	581	0.1	-4.6	1068	0.1	-4.5	1181

Figure 41: Resistance measurements. Part 2

week	25		week	27		week	28				
02.11.2017			13.11.2017			22.11.2017			29.11.2017		
Frequency [kHz]	Angle [deg]	Resistance [kΩ]	Frequenzy [kHz]	Angle [deg]	Resistance [kΩ]	Frequency [kHz]	Angle [deg]	Resistance [kΩ]	Frequenzy [kHz]	Angle [deg]	Resistance [kΩ]
1	-2.5	43.56	1	-2.5	46.87	1	-2.5	48.41	1	-2.5	50.56
1	-2.8	47.13	1	-2.7	50.94	1	-2.8	52.54	1	-2.7	54.79
1	-2.6	45.73	1	-2.5	49.15	1	-2.7	50.49	1	-2.5	52.79
1	-3.6	43.21	1	-3.4	43.02	1	-3.4	43.23	1	-3.4	44.24
1	-3.5	42.66	1	-3.3	42.63	1	-3.3	42.72	1	-3.4	43.25
1	-4.1	44.02	1	-3.9	45.5	1	-4	46.06	1	-3.9	47.37
0.1	-3	92.68	0.1	-3	103.72	0.1	-3	109.86	0.1	-3.1	116.94
0.1	-2.8	102.98	0.1	-2.8	114.43	0.1	-3.3	126.53	0.1	-3.3	134.73
0.1	-2.7	93.04	0.1	-2.7	103.71	0.1	-2.7	108.83	0.1	-2.6	115.24
0.1	-0.1	2640	0.1	-0.1	2686	0.1	-0.1	2851	0.1	-0.1	3102
0.1	-0.1	2558	0.1	-0.1	2590	0.1	-0.1	2767	0.1	-0.1	2986
0.1	-0.1	2636	0.1	-0.1	2700	0.1	-0.1	2852	0.1	-0.2	3040
1	-1.6	3.73	1	-1.6	3.79	1	-1.6	3.8	1	-2.3	3.882
1	-1.3	3.57	1	-1.3	3.64	1	-1.3	3.65	1	-3.3	3.662
1	-1.4	3.49	1	-1.4	3.58	1	-1.4	3.59	1	-1.4	3.67
1	-2.6	8.64	1	-2.6	8.81	1	-2.7	8.83	1	-2.6	9.01
1	-2.6	8.63	1	-2.5	8.83	1	-2.6	8.81	1	-2.5	8.94
1	-2.2	8.25	1	-2.1	8.48	1	-2.3	8.44	1	-2.2	8.61
1	-1.4	21.66	1	-1.2	23.77	1	-1.5	25.09	1	-1.5	26.77
1	-1.6	16.69	1	-1.5	18.43	1	1.8	19.44	1	-1.5	20.66
1	-1.1	14.19	1	-1	15.65	1	-1.2	16.47	1	-1.1	17.52
0.1	-4.6	1431	0.1	-4	1472	0.1	-6	1540	0.1	-7	1632
0.1	-4.6	1345	0.1	-3.9	1399	0.1	-4.2	1473	0.1	-4.3	1568
0.1	-5.3	1310	0.1	-4.9	1480	0.1	-6.4	1621	0.1	-8.5	1811

Figure 42: Resistance measurements. Part 3

A.5   Error in PF-testing

Table 20: Negative and positive error values in Figure 25

Cement	Exposure	Error	Volume [cm^3]	Initial moisture [Volume %]	Porosity [Volume %]	Deg of sat [%]	Initial moisture [Weight %]
CEM II/B-V	90-5	+	0.106	1.027	0.230	5.083	0.492
		-	0.173	0.703	0.160	3.492	0.335
	60-1	+	0.735	0.034	0.163	0.271	0.010
		-	0.585	0.043	0.130	0.530	0.014
	90-0	+	0.324	0.206	0.302	0.253	0.116
		-	0.387	0.163	0.190	0.247	0.094
	60-0	+	0.238	0.794	0.803	1.551	0.452
		-	0.283	0.413	0.495	0.951	0.243
	Sealed	+	1.727	0.299	0.323	0.162	0.170
		-	1.089	0.209	0.192	0.142	0.124
CEM I	90-5	+	0.095	0.080	0.087	1.018	0.023
		-	0.166	0.111	0.129	0.808	0.028
	60-1	+	0.126	0.106	0.242	0.797	0.054
		-	0.149	0.122	0.227	0.541	0.060
	90-0	+	0.047	0.178	0.206	0.114	0.160
		-	0.059	0.183	0.187	0.093	0.148
	60-0	+	0.073	0.102	0.230	0.587	0.046
		-	0.058	0.077	0.206	1.023	0.043
	Sealed	+	3.722	0.161	0.335	1.292	0.092
		-	5.959	0.184	0.240	1.463	0.102

A.6   TGA

The graphs was obtained through TGA.

- Normalize to sample weight

- 1. der - 30 points

- Weight vs. sample temperature
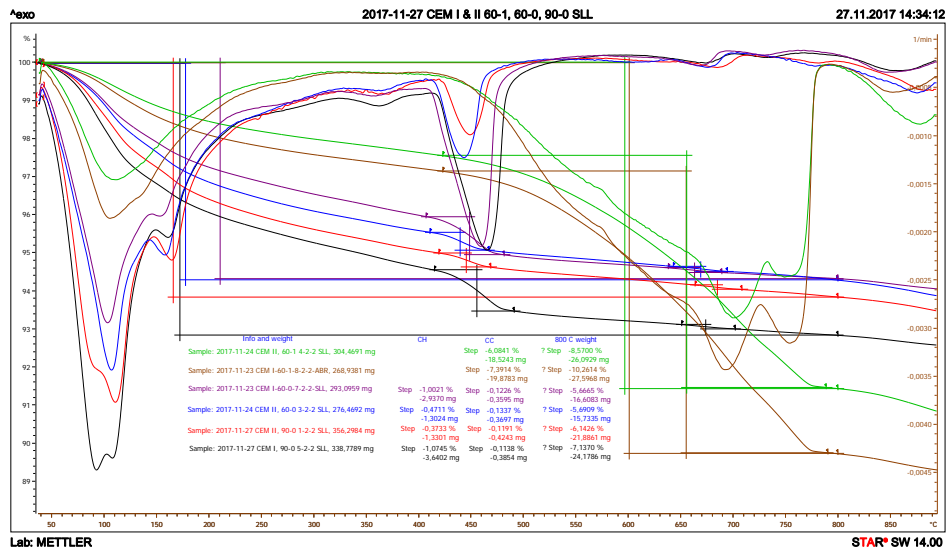
Figure 43: DTG and normalized weight loss of samples from 60-0, 60-1 and 90-0.
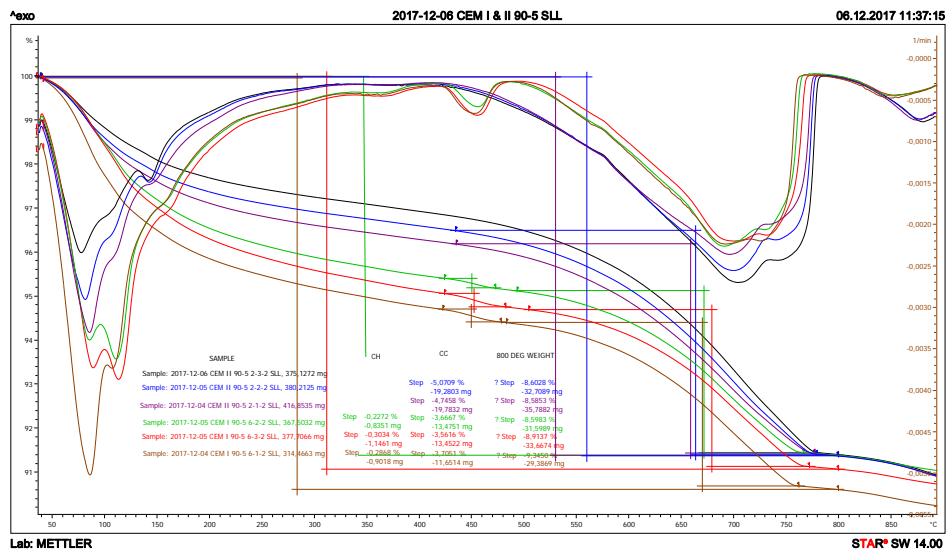
Figure 44: DTG and normalized weight loss of samples from 90-5.

A.7 CWE data

CWE NOTES Simon Liseth Langedal

Samples		1-2-2	1-3-2	1-4-2	3-2-2	3-3-2	3-4-2	4-2-2	4-3-2	4-4-2	5-2-2	5-3-2	5-4-2
Sample name written on bottle		10436701-01	10436701-02	10436701-03	10436701-04	10436701-05	10436701-06	10436701-07	10436701-08	10436701-09	10436701-10	10436701-11	10436701-12
Ground powder (20 g)	m_{powder}	20.015	20.050	20.019	20.040	20.052	20.018	20.035	20.010	20.034	20.027	20.030	20.054
Deionized water (measured) (20 g)	m_{water}	19.969	20.769	20.054	19.891	19.954	20.189	20.012	19.850	19.832	20.022	19.943	19.780
Sample size filtrate (e.g. 10 ml)	$V_{filtrate\ tot}$	11.5	12.5	11	11	11	10.5	11.5	11.5	11	11.5	10.5	11
Amount of used filtrate (e.g. 1ml)	$V_{filtrate}$	1	1	1	1	1	1	1	1	1	1	1	1
Added deionized water (e.g. 9 ml)	$V_{dilution}$	9	9	9	9	9	9	9	9	9	9	9	9
Acidification – added HNO₃ (e.g. 0.14 ml)	V_{acid}	0.14	0.14	0.14	0.14	0.14	0.14	0.14	0.14	0.14	0.14	0.14	0.14
Dilution	D	10.14	10.14	10.14	10.14	10.14	10.14	10.14	10.14	10.14	10.14	10.14	10.14

	Samples	7-2-2	7-3-2	7-4-2	8-2-2	8-3-2	8-4-2	10-3-1	10-4-1	10-5-1	12-3-1	12-4-1	12-5-1
Sample name written on bottles	$m_{powder\ tot}$	10436701-13	10436701-14	10436701-15	10436701-16	10436701-17	10436701-18	10436701-19	10436701-20	10436701-21	10436701-22	10436701-23	10436701-24
Ground powder (20 g)	m_{powder}	20.031	20.057	20.041	20.014	20.035	20.016	20.004	20.007	20.017	19.999	20.038	20.038
Deionized water (measured) (20 g)	m_{water}	20.051	20.022	20.094	19.823	20.037	20.032	19.996	20.026	20.010	20.011	20.028	20.003
Sample size filtrate (e.g. 10 ml)	$V_{filtrate\ tot}$	12	12	12	11.5	11.5	11.5	11	10	12.5	12.5	10	11.5
Amount of used filtrate (e.g. 1ml)	$V_{filtrate}$	1	1	1	1	1	1	1	1	1	1	1	1
Added deionized water (e.g. 9 ml)	$V_{dilution}$	9	9	9	9	9	9	9	9	9	9	9	9
Acidification – added HNO₃ (e.g. 0.14 ml)	V_{acid}	0.14	0.14	0.14	0.14	0.14	0.14	0.14	0.14	0.14	0.14	0.14	0.14
Dilution	D	10.14	10.14	10.14	10.14	10.14	10.14	10.14	10.14	10.14	10.14	10.14	10.14

PSE

Samples	10-1	10-2	11-7	12-2
sample name	10436701-25	10436701-26	10436701-27	10436701-28
cement	CEM I	CEM I	CEM II/B-V	CEM II/B-V
$V_{filtrate}$	1	1	1	1*
$V_{dilution}$	9	9	9	9
V_{acid}	0.14	0.14	0.14	0.14
D	10.14	10.14	10.14	10.14

*amount of pore water was slightly under 1 ml

Figure 45: Weights of $m_{water\ added}$, m_{powder}, dilution and acidification of samples during CWE.

A.8   PF-weight

Figure 46: PF-measurement of samples exposed to CO_2.

Figure 47: PF-measurements of samples stored in desiccators and sealed conditions.

A.9   ICP-MS raw data

Sample	Position					expected results	
10436701-07	4-2-2	Carbonated	CEM II/B-V	60-1	227	154	
10436701-07	4-2-2	Carbonated	CEM II/B-V	60-1	227	154	
10436701-08	4-3-2	Carbonated	CEM II/B-V	60-1	227	154	
10436701-09	4-4-2	Carbonated	CEM II/B-V	60-1	227	154	
10436701-16	8-2-2	Carbonated	CEM I	60-1	181	154	
10436701-17	8-3-2	Carbonated	CEM I	60-1	181	154	
10436701-18	8-4-2	Carbonated	CEM I	60-1	181	154	
10436701-01	1-2-2	Non carbonated	CEM II/B-V	90-0	521	1079	
10436701-01	1-2-2	Non carbonated	CEM II/B-V	90-0	521	1079	
10436701-02	1-3-2	Non carbonated	CEM II/B-V	90-0	521	1079	
10436701-03	1-4-2	Non carbonated	CEM II/B-V	90-0	521	1079	
10436701-04	3-2-2	Non carbonated	CEM II/B-V	60-0	521	1079	
10436701-05	3-3-2	Non carbonated	CEM II/B-V	60-0	521	1079	
10436701-06	3-4-2	Non carbonated	CEM II/B-V	60-0	521	1079	
10436701-10	5-2-2	Non carbonated	CEM I	90-0	794	1542	79
10436701-11	5-3-2	Non carbonated	CEM I	90-0	794	1542	79
10436701-12	5-4-2	Non carbonated	CEM I	90-0	794	1542	79
10436701-13	7-2-2	Non carbonated	CEM I	60-0	794	1542	79
10436701-14	7-3-2	Non carbonated	CEM I	60-0	794	1542	79
10436701-15	7-4-2	Non carbonated	CEM I	60-0	794	1542	79
10436701-19	10-3-1	Non carbonated	CEM II/B-V	Sealed	521	1079	
10436701-20	10-4-1	Non carbonated	CEM II/B-V	Sealed	521	1079	
10436701-21	10-5-1	Non carbonated	CEM II/B-V	Sealed	521	1079	
10436701-22	12-3-1	Non carbonated	CEM I	Sealed	794	1542	79
10436701-23	12-4-1	Non carbonated	CEM I	Sealed	794	1542	79
10436701-24	12-5-1	Non carbonated	CEM I	Sealed	794	1542	79

Isotope	Mo98(MR)		Sn118(LR)		Pb208(LR)		U238
Parameters / Sample ID	Conc. µg/L	RSD %	Conc. µg/L	RSD %	Conc. µg/L	RSD %	Conc. µg/L
Start statistical calculations							
Simon-langland-1-24-7	125.9	0.9	0.017	23.8	0.008	11.1	0.0001
Repeat-langtest-131	127.2	0.6	0.016	4.6	0.018	1.7	0.0004
Simon-langland-1-24-8	127.9	4.2	0.016	1.0	0.013	5.0	0.0005
Simon-langland-1-24-9	137.6	0.4	0.014	7.5	0.016	6.0	0.0000
Simon-langland-1-24-17	145.0	2.5	0.019	6.4	0.013	12.5	0.0005
Simon-langland-1-24-16	172.3	2.4	0.022	14.7	0.021	4.0	0.0011
Simon-langland-1-24-18	146.9	2.3	0.015	22.8	0.015	0.7	0.0001
Simon-langland-1-24-1	29.2	0.6	0.021	24.1	0.038	10.4	0.0000
Repeat-langtest-132	29.5	1.9	0.019	20.3	0.038	8.5	0.0000
Simon-langland-1-24-2	28.4	1.2	0.019	22.2	0.057	4.6	0.0000
Simon-langland-1-24-3	26.7	4.3	0.018	13.7	0.057	3.4	0.0001
Simon-langland-1-24-4	40.8	1.7	0.020	22.2	0.034	2.1	0.0001
Simon-langland-1-24-5	42.1	4.0	0.020	12.6	0.031	15.0	-0.0001
Simon-langland-1-24-6	38.6	3.3	0.016	7.4	0.033	6.8	0.0002
Simon-langland-1-24-10	41.0	1.4	0.018	6.6	0.059	2.9	0.0002
Simon-langland-1-24-11	41.3	2.9	0.021	7.9	0.059	9.3	0.0004
Simon-langland-1-24-12	38.5	3.1	0.020	19.3	0.060	2.3	0.0000
Simon-langland-1-24-13	65.0	3.1	0.016	21.5	0.050	0.6	0.0002
Simon-langland-1-24-14	63.9	3.1	0.024	17.5	0.057	4.0	0.0002
Simon-langland-1-24-15	65.7	1.5	0.018	18.8	0.051	9.1	0.0002
Simon-langland-1-24-19	22.5	0.4	0.020	11.9	0.104	9.1	0.0002
Simon-langland-1-24-20	23.7	2.8	0.077	8.9	0.117	3.8	0.0003
Simon-langland-1-24-21	22.0	3.1	0.025	12.9	0.090	2.0	0.0002
Simon-langland-1-24-22	21.4	2.8	0.016	18.5	0.076	6.5	0.0002
Simon-langland-1-24-23	28.2	1.2	0.021	5.3	0.069	6.2	0.0001
Simon-langland-1-24-24	24.7	3.1	0.022	17.7	0.075	3.3	0.0002
Stop statistical calculations							
Average	64.46	2.3	0.019	14.2	0.048	5.8	0.0002
Min	21.41	0.4	0.014	1.0	0.008	0.6	-0.0001
Max	172.29	4.3	0.025	24.1	0.117	15.0	0.0011
Std	49.27	1.2	0.003	6.9	0.029	3.8	0.0002
Rsd % <5, 5-10, >10	76.4	0.5	15.1		60.0		109.0
Confidence interval 95%	19.71		0.001		0.012		0.0001
Confidence interval 95% (%) <5, 5-10, >10	30.6		6.0		24.0		43.6
Number	26	26	26	26	26	26	26

Figure 48: Raw data from ICP-MS analysis. Batch 1 part 1.

Figure 49: Raw data from ICP-MS analysis. Batch 1 part 2.

Cr53(MR) Conc. µg/L	RSD %	Mn55(MR) Conc. µg/L	RSD %	Fe56(MR) Conc. µg/L	RSD %	Ni60(MR) Conc. µg/L	RSD %	Cu63(MR) Conc. µg/L	RSD %	Zn66(MR) Conc. µg/L	RSD %	Rb85(MR) Conc. µg/L	RSD %	Sr88(MR) Conc. µg/L	RSD %	Sn121(MR) Conc. µg/L	RSD %
33.17	1.7	0.014	25.1	4.00	2.6	0.16	20.8	1.84	2.0	0.21	22.7	10.3	0.6	69.0	1.4	2.266	1.2
32.83	2.1	0.014	27.9	3.81	2.3	0.16	21.7	1.79	4.1	0.21	12.4	10.3	0.7	66.8	0.4	2.317	1.3
31.67	1.1	0.023	32.5	3.71	1.6	0.18	55.7	1.36	3.3	0.21	21.8	9.5	1.3	65.2	2.0	2.274	2.3
33.44	2.6	0.026	11.4	2.30	3.3	0.41	43.1	1.79	3.4	0.22	7.1	14.4	0.9	72.4	3.0	2.375	5.6
53.93	1.9	0.012	21.4	15.07	2.5	0.16	12.1	2.05	2.0	0.11	9.1	13.4	2.5	73.3	2.8	0.060	11.4
65.04	3.7	0.035	21.4	16.64	3.8	0.21	29.8	8.00	2.1	1.63	2.7	14.5	2.1	78.4	2.5	0.137	14.7
54.30	2.0	0.017	29.9	13.38	2.2	0.17	19.2	1.87	8.0	0.14	42.4	14.0	2.5	69.8	0.4	0.050	21.2
3.28	0.7	0.015	10.7	4.81	1.0	0.14	30.4	2.26	3.0	0.67	4.9	327.4	1.4	649.3	1.3	0.050	23.2
3.27	2.6	0.015	11.3	4.84	2.3	0.15	28.9	2.09	3.2	0.74	10.6	336.8	2.0	678.1	1.3	0.030	24.8
2.61	1.0	0.007	38.5	5.78	4.5	0.08	40.9	3.16	0.7	1.47	6.1	353.0	2.8	634.1	2.4	0.046	45.0
2.57	4.5	0.002	14.5	6.32	2.3	0.08	49.4	3.12	3.2	0.87	5.5	403.4	3.2	650.6	4.3	0.039	17.3
2.55	2.1	0.014	23.4	3.14	2.0	0.09	46.8	1.57	4.2	0.45	5.2	304.9	1.0	480.6	0.4	0.054	32.0
2.82	1.2	0.015	1.6	2.76	0.1	0.07	46.2	2.00	8.5	0.49	8.7	328.1	1.0	505.0	1.3	0.032	30.6
1.88	8.0	0.019	29.9	2.65	6.6	0.12	30.5	1.42	0.4	0.41	20.7	285.3	1.3	454.3	0.5	0.031	21.3
4.26	1.7	0.007	7.3	1.82	1.5	0.20	19.6	3.48	1.6	1.21	7.7	396.2	2.1	1,060.7	0.3	0.041	47.7
2.81	6.7	0.013	23.4	2.25	7.2	0.19	14.8	4.47	6.2	1.13	20.5	424.7	0.4	987.3	8.3	0.025	22.0
2.51	4.2	0.016	22.1	2.46	7.4	0.25	16.5	4.38	5.2	1.15	10.1	392.0	1.0	983.3	3.5	0.034	20.6
1.65	3.1	0.006	11.0	3.72	2.5	0.19	20.2	2.77	3.6	0.63	16.9	370.1	2.4	817.3	2.1	0.025	16.6
1.70	0.4	0.010	13.3	0.59	1.2	0.19	13.3	2.92	3.0	0.82	9.6	365.7	0.5	801.4	5.2	0.033	83.9
1.96	0.4	0.005	16.2	0.97	4.2	0.17	35.4	2.69	5.0	0.53	12.0	359.0	1.4	805.3	2.2	0.014	51.7
1.41	3.8	0.011	19.0	6.23	1.3	0.09	22.6	2.63	7.1	0.59	13.6	395.0	3.9	846.4	3.9	0.077	14.1
1.55	5.0	0.010	8.5	8.47	2.8	0.05	53.9	3.72	3.4	1.00	11.5	453.6	0.5	753.5	5.2	0.068	35.0
1.42	1.5	0.017	13.8	6.71	1.3	0.05	30.0	1.45	5.5	0.68	18.1	440.6	0.4	863.7	1.7	0.078	42.2
1.47	6.3	0.010	11.6	1.13	0.3	0.16	13.3	3.02	4.5	0.71	17.0	418.6	3.0	1,220.1	6.8	0.023	24.0
1.57	3.2	0.010	12.0	1.86	1.5	0.20	21.2	2.58	6.5	0.66	5.7	414.4	2.4	1,063.6	3.9	0.028	15.6
1.65	8.0	0.016	5.7	1.56	5.5	0.23	13.0	2.90	4.5	0.76	16.7	416.9	1.4	1,052.0	5.0	0.022	30.1
26	26	26	26	26	26	26	26	26	26	26	26	26	26	26	26	26	26
59.4	0.9	19.9	3.7	34.7	0.8	19.0	5.4	20.0	0.8	23.8	3.3	24.3	0.4	25.0	0.8	84.7	7.3
7.94		0.003		1.70		0.03		0.55		0.16		68.01		152.1		0.333	
148.6	2.2	48.6	9.2	86.8	2.0	47.5	13.6	50.0	2.1	59.4	8.3	60.9	1.0	62.6	2.1	2111.8	
19.85		0.007		4.24		0.08		1.37		0.40		170.02		380.4		0.833	18.2

Figure 50: Raw data from ICP-MS analysis. Batch 1 part 3.

ification of your samples , linked to Project-number, choose your
ld of Heading 1 - 4, replace it with heading suitable for you project

main elements (insert more column if needed

High concentration of

Date of analyses: 13.12.17 selvens 121

Counting digits = 3

Sample name	Sample name	Carb/non carb	Cement type	RH - CO2	Na	K	Ca
						> 150 mg/l	
10436701 - 25	10-1	Non carbonated	CEM II/B-V	Sealed - PSE	521	1 079	
10436701 - 25	10-1	Non carbonated	CEM II/B-V	Sealed - PSE	521	1 079	
10436701 - 26	10-2	Non carbonated	CEM II/B-V	Sealed - PSE	521	1 079	
10436701 - 27	11-7	Non carbonated	CEM I	Sealed - PSE	794	1 542	79
10436701 - 28	12-2	Non carbonated	CEM I	Sealed - PSE	794	1 542	79
10436701 - 29	2-1-2	Carbonated	CEM II/B-V	90-5	227	154	
10436701 - 30	2-2-2	Carbonated	CEM II/B-V	90-5	227	154	
10436701 - 31	2-3-2	Carbonated	CEM II/B-V	90-5	227	154	
10436701 - 32	6-1-2	Partly carbonated	CEM I	90-5	794	1 542	79
10436701 - 33	6-2-2	Partly carbonated	CEM I	90-5	794	1 542	79
10436701 - 34	6-3-2	Partly carbonated	CEM I	90-5	794	1 542	79
10436701 - 35	9-4	Carbonated	CEM II/B-V	60-100	227	154	
10436701 - 36	9-5	Carbonated	CEM II/B-V	60-100	227	154	
10436701 - 37	9-6	Carbonated	CEM II/B-V	60-100	227	154	
10436701 - 38	11-4	Carbonated	CEM I	60-100	181	154	
10436701 - 39	11-5	Carbonated	CEM I	60-100	181	154	
10436701 - 40	11-6	Carbonated	CEM I	60-100	181	154	

Sample ID	Parameteres Isotope	L7(LR) Conc. µg/L	RSD. %	B11(LR) Conc. µg/L	RSD. %	Y89 Conc. µg/L
Start statistical calculations						
Langedal25-40-25		855.44	0.9	4.0	0.6	0.0054
Repeatingtest-205		771.80	7.7	4.0	4.3	0.0039
Langedal25-40-26		777.08	1.1	7.9	3.6	0.0031
Langedal25-40-27		202.12	0.7	6.4	2.0	0.0043
Langedal25-40-28		142.76	2.9	4.5	0.5	0.0170
Langedal25-40-29		18.97	1.7	22.4	1.5	0.0031
Langedal25-40-30		18.70	2.6	32.7	2.1	0.0030
Langedal25-40-31		19.69	0.9	47.0	0.9	0.0026
Langedal25-40-32		4.07	0.8	2.4	2.1	0.0037
Langedal25-40-33		3.79	1.2	1.4	3.4	0.0032
Langedal25-40-34		3.78	2.5	1.0	2.7	0.0038
Langedal25-40-35		53.33	1.1	207.8	3.1	0.0038
Langedal25-40-36		48.70	1.8	175.5	5.7	0.0032
Langedal25-40-37		48.18	1.4	174.2	2.9	0.0030
Langedal25-40-38		18.44	4.1	34.9	2.6	0.0027
Langedal25-40-39		18.90	4.8	30.6	4.0	0.0036
Langedal25-40-40		19.19	1.5	28.6	1.4	0.0028
Stop statistical calculations						
Average		177.94	2.2	46.2	2.6	0.0042
Min		3.78	0.7	1.0	0.5	0.0026
Max		855.44	7.7	207.8	5.7	0.0170
Std		302.49	1.8	68.4	1.4	0.0034
Rsd % <5, 5-10, >10		170.0		148.2		73.0
Confidence interval 95%		151.25	0.9	34.2	0.7	0.0017
Confidence interval 95% (%) <5, 5-10, >10		85.0		74.1		39.5
Number		17	17	17	17	17

Figure 51: Raw data from ICP-MS analysis. Batch 2 part 1.

(LR) RSD %	Mo98(MR) Conc. µg/L	RSD %	Sn118(LR) Conc. µg/L	RSD %	Ce140(LR) Conc. µg/L	RSD %	Pr141(LR) Conc. µg/L	RSD %	W182(LR) Conc. µg/L	RSD %	Tl205(LR) Conc. µg/L	RSD %	Pb208(LR) Conc. µg/L	RSD %	U238(LR) Conc. µg/L	RSD %
22.8	513.32	3.0	0.514	3.2	0.007	19.5	0.0006	9.0	2.814	1.6	0.0050	15.7	2.509	0.9	0.0016	23.6
23.8	487.88	1.4	0.510	4.7	0.007	1.8	0.0012	18.2	2.786	1.0	0.0043	22.4	2.434	3.2	0.0013	30.2
16.0	524.46	1.3	1.301	0.8	0.007	13.4	0.0011	19.0	4.120	2.0	0.0026	2.3	1.829	3.4	0.0031	8.8
21.0	454.65	2.2	1.374	2.1	0.006	11.1	0.0006	46.5	1.236	3.6	0.0028	18.6	4.765	1.4	0.0101	2.9
5.4	427.07	0.9	1.523	3.3	0.041	2.8	0.0053	20.9	1.044	4.3	0.0020	54.7	5.090	1.5	0.0140	20.6
26.2	164.35	1.7	0.028	4.9	0.004	24.7	0.0008	31.8	0.806	1.8	0.0048	34.0	0.026	6.2	0.0003	49.9
62.5	180.15	4.7	0.023	25.0	0.004	14.0	0.0007	50.5	1.247	2.4	0.0064	18.9	0.027	5.7	0.0010	7.7
47.8	190.38	3.5	0.020	20.8	0.004	13.6	0.0003	63.5	1.669	0.9	0.0071	4.3	0.021	11.7	0.0006	14.8
16.5	46.17	1.3	0.022	5.5	0.002	30.1	0.0005	48.2	0.049	9.6	0.0027	9.7	0.057	9.3	0.0004	30.2
33.4	49.53	2.4	0.027	28.9	0.002	28.2	0.0002	28.2	0.036	14.4	0.0023	48.8	0.040	5.2	0.0001	25.8
22.4	42.09	0.3	0.026	22.8	0.003	20.4	0.0006	24.1	0.035	11.6	0.0021	42.5	0.037	7.5	0.0003	57.1
22.0	234.25	2.3	0.026	7.9	0.004	25.8	0.0009	12.1	2.969	4.5	0.0142	12.9	0.133	3.9	0.3945	2.6
17.7	208.59	1.3	0.015	10.9	0.004	27.0	0.0004	173.2	2.833	5.4	0.0136	7.6	0.117	7.7	0.3294	7.2
9.1	217.34	3.2	0.021	14.7	0.004	8.0	0.0004	87.4	2.896	4.2	0.0145	5.7	0.542	2.3	0.3377	3.7
37.0	428.93	2.9	0.021	14.2	0.004	2.0	0.0005	56.0	3.027	1.2	0.0067	12.0	0.019	8.8	0.0023	12.9
38.2	423.68	0.4	0.019	16.0	0.003	2.4	0.0009	33.4	2.974	2.9	0.0035	13.2	0.019	5.3	0.0013	22.3
13.7	409.60	3.1	0.024	25.5	0.003	44.9	0.0007	46.9	2.996	3.5	0.0029	11.8	0.015	9.9	0.0012	50.5
25.6	294.26	2.1	0.323	12.4	0.006	17.0	0.0009	45.2	1.973	4.4	0.0057	19.7	1.040	5.5	0.0647	218.8
5.4	42.09	0.3	0.015	0.8	0.002	1.8	0.0002	9.0	0.035	0.9	0.0020	2.3	0.015	0.9	0.0001	2.6
62.5	524.46	4.7	1.523	28.9	0.041	44.9	0.0053	173.2	4.120	14.4	0.0145	54.7	5.090	11.7	0.3945	57.1
14.4	171.87	1.2	0.539	9.3	0.009	12.1	0.0012	38.8	1.283	3.9	0.0043	15.8	1.698	3.3	0.1386	17.3
58.4	58.4		166.9		145.2		126.1		65.0		75.0		163.3		214.3	
7.2	85.93	0.6	0.270	4.7	0.005	6.1	0.0006	19.4	0.641	1.9	0.0022	7.9	0.849	1.6	0.0693	8.6
	29.2		83.5		72.6		63.1		32.5		37.5		81.6		107.2	
17	17	17	17	17	17	17	17	17	17	17	17	17	17	17	17	17

Figure 52: Raw data from ICP-MS analysis. Batch 2 part 2.

	Na23(MR)		Mg25(MR)		Al27(MR)		Si29(MR)		P31(MR)		S34(MR)		Cl35(MR)		K39(MR)		Ca44
	Conc. µg/L	RSD %	Conc. µg/L	RSD %	Conc. µg/L	RSD %	Conc. µg/L	RSD %	Conc. µg/L	RSD %	Conc. µg/L	RSD %	Conc. µg/L	RSD %	Conc. µg/L	RSD %	Conc. µg/L
	287 394	3.5	2.1	6.7	1 934.8	1.6	968	1.0	10.5	1.4	5 997	2.1	4 139	2.0	579 771	3.5	2 545
	260 682	5.0	1.8	3.5	1 779.6	5.8	872	1.8	9.8	7.5	5 471	1.4	4 508	0.9	548 850	1.5	2 319
	264 270	3.3	4.3	2.5	2 245.3	0.3	1 194	1.2	13.6	4.3	6 657	2.9	5 632	7.4	543 462	2.5	1 804
	611 077	2.6	2.2	5.7	502.8	2.0	1 181	1.0	21.0	2.6	23 866	2.1	4 870	2.8	1 204 040	2.6	3 733
	511 583	2.1	16.2	5.5	432.1	1.9	1 660	1.6	33.7	1.8	25 793	2.3	5 099	1.5	1 073 170	3.7	2 433
	15 078	5.3	38.9	3.7	44.9	2.3	1 138	1.4	4.1	8.1	46 972	0.4	4 986	3.6	14 922	5.3	47 335
	13 481	6.6	179.7	2.3	14.6	12.1	1 396	1.3	5.1	3.3	58 178	6.0	5 035	1.5	10 528	8.4	62 933
	12 352	4.4	629.9	6.2	6.7	2.5	1 458	0.8	4.3	6.1	62 494	1.3	5 715	2.2	8 855	5.1	64 620
	22 872	9.0	4.2	5.6	39.7	5.6	143	1.1	4.3	2.4	1 046	7.0	3 026	6.2	39 582	5.6	31 553
	20 725	2.4	3.7	7.2	36.0	0.6	159	1.3	4.4	3.6	1 146	3.2	2 772	1.1	34 154	6.1	34 895
	21 434	1.9	4.5	5.6	30.6	1.5	110	0.8	3.6	5.2	1 031	0.8	2 763	0.8	37 235	1.3	32 320
	10 674	3.3	17 719.6	3.0	4.7	5.6	513	0.1	6.2	5.1	65 686	4.0	6 044	3.1	8 704	4.8	47 247
	9 356	1.4	15 468.1	3.6	4.0	7.2	390	1.1	4.5	5.5	56 195	3.4	5 380	4.6	6 852	2.7	42 850
	9 541	4.7	15 644.1	3.0	4.4	9.1	406	1.4	5.4	2.0	59 608	1.5	5 583	2.6	6 825	5.2	45 639
	13 375	6.0	2 925.2	1.6	8.7	2.8	1 001	0.9	5.6	4.5	59 266	1.8	7 994	3.2	9 283	3.6	60 297
	12 960	7.7	3 560.9	6.1	8.5	6.4	1 039	2.7	6.3	4.7	57 973	4.3	7 971	0.8	8 831	10.5	55 341
	13 088	3.8	3 790.5	2.2	9.8	2.8	1 032	0.7	5.6	1.8	57 455	1.2	7 427	8.5	8 815	3.1	54 567
	124 114	4.3	3 529	4.4	418.1	4.1	862	1.2	8.7	4.1	34 990	2.7	5 232	3.1	243 757	4.4	34 849
	9 366	1.4	2	1.6	4.0	0.3	110	0.1	3.6	1.4	1 031	0.4	2 763	0.8	6 825	1.3	1 804
	611 077	9.0	17 720	7.2	2 245.3	12.1	1 660	2.7	33.7	8.1	65 686	7.0	7 994	8.5	1 204 040	10.5	64 620
	193 072	2.1	6 236	1.8	767.6	3.3	486	0.5	7.8	2.0	26 495	1.8	1 584	2.3	397 568	2.4	23 520
	155.6		176.7		183.6		56.4		90.0		75.7		30.3		163.1		67.5
	77.8	1.1	88.4	0.9	91.8	1.6	28.2	0.3	45.0	1.0	37.9	0.9	15.1	1.2	81.5	1.2	33.7
	96 536		3 118		383.8		243		3.9		13 247		792		198 784		11 760
	17	17	17	17	17	17	17	17	17	17	17	17	17	17	17	17	17

Figure 53: Raw data from ICP-MS analysis. Batch 2 part 3.

	Ti49(MR)		V51(MR)		Cr53(MR)		Mn55(MR)		Fe56(MR)		Co59(MR)		Ni60(MR)		Cu63(MR)	
(MR)	RSD %	Conc. µg/L	RSD %	Conc. µg/L	RSD %	Conc. µg/L	RSD %	Conc. µg/L	RSD %	Conc. µg/L	RSD %	Conc. µg/L	RSD %	Conc. µg/L	RSD %	Conc. µg/L
	3.5	0.71	12.9	1.60	4.2	9.75	1.7	0.52	5.0	623.50	1.2	1.815	7.6	3.04	2.5	109.49
	1.9	0.65	7.5	1.40	5.8	9.40	1.2	0.53	4.3	589.13	1.0	1.824	5.1	2.98	0.7	102.39
	0.9	1.11	0.5	2.68	5.8	10.22	2.9	1.25	1.4	727.91	0.8	2.153	4.3	6.01	2.2	78.45
	2.7	1.43	13.3	2.22	4.0	59.90	0.5	1.39	0.7	108.15	2.0	21.745	1.0	8.75	1.4	96.49
	1.9	3.53	6.3	2.76	6.4	50.93	2.3	2.85	4.6	154.08	0.4	20.254	1.8	9.97	2.6	117.50
	5.7	0.20	20.7	1.23	5.9	3.17	13.0	0.06	11.6	10.63	2.2	0.470	17.6	0.09	4.1	4.79
	4.2	0.22	11.7	2.04	3.5	10.55	7.8	0.14	14.9	15.80	3.5	0.296	27.9	0.15	4.1	3.08
	3.4	0.15	17.3	2.47	4.9	12.03	1.0	0.06	12.9	5.65	4.3	0.161	12.6	0.13	3.1	2.55
	4.5	0.09	50.9	0.02	47.2	0.23	5.6	0.04	6.9	9.02	1.4	1.564	9.1	0.14	1.6	3.93
	3.2	0.10	37.5	0.01	54.2	0.42	15.2	0.05	26.2	8.46	3.1	1.727	26.1	0.15	5.7	4.23
	2.5	0.16	24.3	0.01	15.1	0.30	8.3	0.03	33.1	9.16	2.4	1.712	27.5	0.15	5.3	2.33
	1.8	0.27	13.7	0.77	7.0	0.69	12.3	1.82	3.6	4.75	7.3	0.138	7.4	1.18	5.9	1.79
	2.8	0.23	8.5	0.66	1.5	0.74	10.3	1.35	2.4	4.37	1.8	0.141	22.0	0.80	4.9	3.96
	1.6	0.22	63.5	0.72	5.3	0.75	2.1	1.41	3.6	7.35	16.5	0.126	8.9	1.04	2.2	5.00
	1.4	0.18	34.6	1.82	4.2	70.94	2.2	0.12	18.1	15.46	6.2	0.233	22.2	0.30	1.2	10.55
	9.8	0.22	28.2	1.95	3.5	75.94	2.8	0.11	19.8	13.78	2.9	0.173	4.0	0.33	2.1	5.19
	2.4	0.16	46.4	2.01	1.8	48.21	1.2	0.07	29.6	13.39	1.6	0.173	3.3	0.29	1.7	4.24
	3.2	0.57	23.4	1.43	10.6	21.42	5.3	0.69	11.7	136.51	3.4	3.218	7.2	2.09	3.0	32.70
	0.9	0.09	0.5	0.01	1.5	0.23	0.5	0.03	0.7	4.37	0.4	0.126	0.9	0.09	0.7	1.79
	9.8	3.53	63.5	2.76	54.2	75.94	15.2	2.85	33.1	727.91	16.5	21.745	27.9	9.97	5.9	117.50
	2.1	0.85	17.7	0.93	15.4	27.45	4.8	0.84	10.4	248.20	3.8	6.741	9.5	3.16	1.7	45.99
	75.4	150.7	32.4	64.7	64.1	128.2	60.1	120.2	90.9	181.8	104.8	209.5	75.6	151.2	70.3	140.6
	1.1	0.43	8.9	0.46	7.7	13.73	2.4	0.42	5.2	124.10	1.9	3.371	4.8	1.58	0.8	22.99
	17	17	17	17	17	17	17	17	17	17	17	17	17	17	17	17

Figure 54: Raw data from ICP-MS analysis. Batch 2 part 4.

Cu65(MR) Conc. µg/L	RSD %	Zn66(MR) Conc. µg/L	RSD %	Rb85(MR) Conc. µg/L	RSD %	Sr88(MR) Conc. µg/L	RSD %	Sb121(MR) Conc. µg/L	RSD %	Ba137(MR) Conc. µg/L	RSD %	As75(HR) Conc. µg/L	RSD %
107.81	1.2	51.93	1.4	2'736.43	1.7	166.1	1.3	0.756	7.4	15.19	5.4	1.62	8.2
101.47	1.4	50.13	3.7	2'610.54	1.6	159.4	1.1	0.666	8.7	14.27	1.5	1.54	10.0
80.33	1.6	59.33	1.1	2'658.16	1.1	79.7	1.7	0.701	11.9	5.08	7.0	3.63	9.6
96.91	2.0	118.59	1.2	5'559.46	2.1	368.8	0.8	0.496	11.3	25.98	3.1	5.16	6.4
116.45	1.8	357.95	0.9	4'733.02	1.8	211.4	1.2	0.530	3.4	12.04	3.8	4.66	2.6
4.60	5.7	0.62	3.2	28.94	4.1	184.9	3.8	0.179	5.9	12.09	1.2	0.03	15.1
3.17	6.1	0.38	20.4	18.47	2.6	181.2	6.3	0.752	12.9	8.06	4.3	0.04	22.3
2.37	2.9	0.30	17.8	14.05	1.0	161.8	0.4	1.422	9.7	6.26	2.3	0.05	60.1
4.07	5.2	1.14	6.3	97.40	2.5	285.4	1.9	0.011	32.7	26.14	3.1	0.02	60.0
3.97	4.6	0.65	8.9	85.50	1.4	251.3	2.0	0.002	86.6	27.72	2.7	0.03	22.9
2.09	5.6	0.68	9.4	92.61	0.8	288.5	1.4	0.009	86.6	29.95	1.4	0.03	21.7
1.60	2.9	0.62	8.5	18.01	1.4	119.9	1.3	3.926	1.6	9.84	1.5	0.24	26.3
3.85	8.7	0.76	12.7	10.31	2.9	102.9	3.8	3.161	2.4	8.11	2.4	0.18	9.5
5.02	4.3	1.65	9.2	9.98	1.6	103.8	2.7	3.262	5.4	8.40	11.2	0.16	15.7
10.36	1.6	0.68	14.4	12.40	3.6	185.9	1.3	1.375	5.4	8.60	1.1	0.04	33.3
5.19	2.3	0.71	5.0	12.35	2.0	177.2	1.9	1.409	6.8	8.11	8.9	0.04	30.1
3.84	4.5	0.45	22.0	12.18	3.0	163.8	4.3	1.343	1.4	7.34	0.3	0.04	53.9
32.53	3.7	38.03	8.6	1'100.58	2.1	187.8	2.2	1.176	17.7	13.72	3.6	1.03	24.0
1.60	1.2	0.30	0.9	9.98	0.8	79.7	0.4	0.002	1.4	5.08	0.3	0.02	2.6
116.45	8.7	357.95	22.0	5'559.46	4.1	368.8	6.3	3.926	86.6	29.95	11.2	5.16	60.1
45.82	2.1	88.86	6.8	1'839.06	0.9	75.1	1.5	1.195	26.9	8.32	3.0	1.74	18.4
140.8	1.1	233.6	3.4	167.1	0.5	40.0	0.8	101.6	13.5	60.7	1.5	169.3	9.2
22.91		44.43		919.53		37.6		0.597		4.16		0.87	
70.4		116.8		83.5		20.0		50.8		30.3		84.7	
17	17	17	17	17	17	17	17	17	17	17	17	17	17

Figure 55: Raw data from ICP-MS analysis. Batch 2 part 5.